AMERICAN UNIVERSITY OF BEIRUT

WICKING RATES IN ELECTRONIC CIGARETTES

by
OMAR MOHAMMED EL HAJJ

A thesis
submitted in partial fulfillment of the requirements
for the degree of Master of Engineering, major Mechanical Engineering
to the Department of Mechanical Engineering
of the Maroun Semaan Faculty of Engineering and Architecture
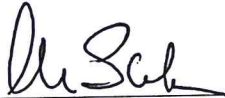at the American University of Beirut

Beirut, Lebanon
December 2018

AMERICAN UNIVERSITY OF BEIRUT

WICKING RATES IN ELECTRONIC CIGARETTES

by
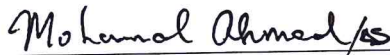OMAR MOHAMMED EL HAJJ

Approved by:

_____

Dr. Alan Shihadeh, Professor   Advisor
Department of Mechanical Engineering

_____

Dr. Kamel Abu Ghali, Professor   Co-Advisor/Member of Committee
Department of Mechanical Engineering

_____

Dr. Mohammad Ahmad, Professor   Member of Committee
Department of Chemical Engineering

Date of thesis/dissertation defense: December 7, 2018

AMERICAN UNIVERSITY OF BEIRUT

THESIS, DISSERTATION, PROJECT RELEASE FORM

Student Name:

El Hajj   Omar   Mohammed

Last   First   Middle

● Master's Thesis   ○ Master's Project   ○ Doctoral Dissertation

☐   I authorize the American University of Beirut to: (a) reproduce hard or electronic copies of my thesis, dissertation, or project; (b) include such copies in the archives and digital repositories of the University; and (c) make freely available such copies to third parties for research or educational purposes.

☑   I authorize the American University of Beirut, to: (a) reproduce hard or electronic copies of it; (b) include such copies in the archives and digital repositories of the University; and (c) make freely available such copies to third parties for research or educational purposes
after:

   One ---- year from the date of submission of my thesis, dissertation, or project.
   Two ---- years from the date of submission of my thesis, dissertation, or project.
   Three ✓ years from the date of submission of my thesis, dissertation, or project.

_____   February 5, 2019

Signature   Date

ACKNOWLEDGMENTS

I would like to thank my advisor, Dr. Alan Shihadeh, for guiding me and helping me reach my potential. Prof. Shihadeh has both the personal and professional attributes that I strive for. I will always consider it a tremendous honor to have studied under his guidance.

I would also like to give thanks and a special acknowledgement to my committee members Dr. Kamel Abou Ghali, who was also my co-advisor, and Dr. Mohamad Ahmad for their valuable input and time.

During the course of this thesis, I met a lot of remarkable people that left a huge impact on my life, these people belong to The Aerosol Group, the different personalities in this group makes it really unique and exceptional. Starting with Nabil Ramlwai and Khairallah Atwi, who were the first people I worked with when I first joined the group. I will never forget the lunch conversations/debates with Nareg Karaoghlanian. The unlimited support and assistant from Mohammed Baasiri, Ebrahim Karam and our lab manager Rola Salman. Last but not least, I wouldn't have done it without the help of Dr. Soha Talih, who did a tremendous effort throughout the whole thesis, particularly the last 3 months, Dr. Talih helped in every part of this thesis.

Finally, a special acknowledgement should be made to my family and friends, who supported me or influenced me along the way. Although it would be impossible to list every name, but some of those that come to mind include Dr. Nagham Ismail, Mohamad Hout, Dr.Mariam Itani, Hisham Ghalayini, Dua Al Assaad and, Walid Abu Hweij.

AN ABSTRACT OF THE THESIS OF

<u>Omar Mohammed El Hajj</u>   for   <u>Master of Engineering</u>
                                      <u>Major</u>: Mechanical Engineering

Title: <u>Wicking Rate in Electronic Cigarettes</u>

Electronic cigarettes (ECIGs) are devices used for nicotine delivery without combusting tobacco. They are marketed as a healthier alternative to regular tobacco cigarettes. While they have become increasingly popular in recent years, with continuously and rapidly evolving product design features and use behaviors, little is known about their safety and effectiveness particularly after volatile carbonyl compounds were detected in ECIG aerosol which are considered a major causative agent in pulmonary disease among tobacco cigarette smokers. These carbonyl compounds are postulated to be the result of what is known as the "Dry Puff", where the heating element dries out and its temperature increases. Design features and user behavior highly influence carbonyl compounds emission and understanding these factors is relevant to regulating these devices.

In this study, the properties of the wicking material used are studied and an experimental method was developed for this purpose, these properties along with principles of heat and mass transfer are plugged into a mathematical model that predict the saturation levels inside the wick or the wick dryness as a function of ECIG design feature and user puffing behavior. The model was run under different scenarios and the results were compared to experimental measurements. The predicted and measured values were strongly correlated, the results also revealed that the different factors affecting saturation levels in the wick were well captured in the mathematical model. Thus, this model can be used to predict the levels of wick dryness that are related to toxic emissions and help guide selection of ECIGs wicking materials, design and use conditions.

CONTENTS

ILLUSTRATIONS

NOMECLATURE

S   Saturation level (dimensionless)

Q   Volumetric flowrate (m^3/s)

A   Cross sectional area (m^2)

L   Length (m)

K   Hydraulic conductivity (cm/s)

h   Hydraulic head (m)

k   Permeability (m^2)

P   Pressure (Pa)

g   Gravitational acceleration (m/s^2)

$\dot{m}$ Mass flowrate (kg/s)

$\dot{Q}$ Heat transfer rate (W)

T   Temperature (K)

V   Volume (m^3)

C_p Specific Heat (J/Kg.K)

K   Thermal Conductivity (W/m.K)

hc   Convective heat transfer coefficient (W/$m^2 K$)

h_{fg} Latent heat of vaporization (J/Kg)

h_m Mass transfer Coefficient (W/$m^2 K$)

M   Molar mass (kg/mol)

Ru   Universal gas constant (J/mol.K)

$\dot{E}$ Electrical power input (Watts)

R   Radius (m)

Greek Letters

θ Contact Angle (degrees)

ρ Density (Kg/m^3)

μ   Viscosity (m^2/s)

γ Surface tension (N/m)

ϵ Porosity (dimensionless)

Subscripts

w   Wetting phase

nw   Non-wetting phase

l Liquid

a   Air

evap.   Evaporated

cond.   Conduction

conv.   Convection

CV   Control Volume

PG   Propylene Glycol

CHAPTER I

INTRODUCTION

Electronic cigarettes are nicotine delivery devices that were introduced to the market in 2004, since then, their global use has increased exponentially [1] with estimated global sales reaching $10 billion in 2017 surpassing conventional cigarettes sales [2] (Fig. 1).

Electronic cigarettes, also called e-cigarettes or ECIGs, are designed to deliver nicotine without burning tobacco by using a heating element powered by a battery that vaporize a liquid into inhalable aerosols, the liquid is usually a mixture of propylene glycol (PG) and/or vegetable glycerin (VG), flavorings, water and nicotine[3]. ECIGs have been in the spotlight for several reasons, including the popular belief that they are a safer alternative to tobacco cigarettes since there is no combustion happening [4], the uncertainty regarding their long term health effects [5], and their consumption by young people. About 2 million middle- and high-school students tried e-cigarettes in 2014, triple the number of teen users in 2013, the Centers for Disease Control and Prevention reported in 2015 [6] .
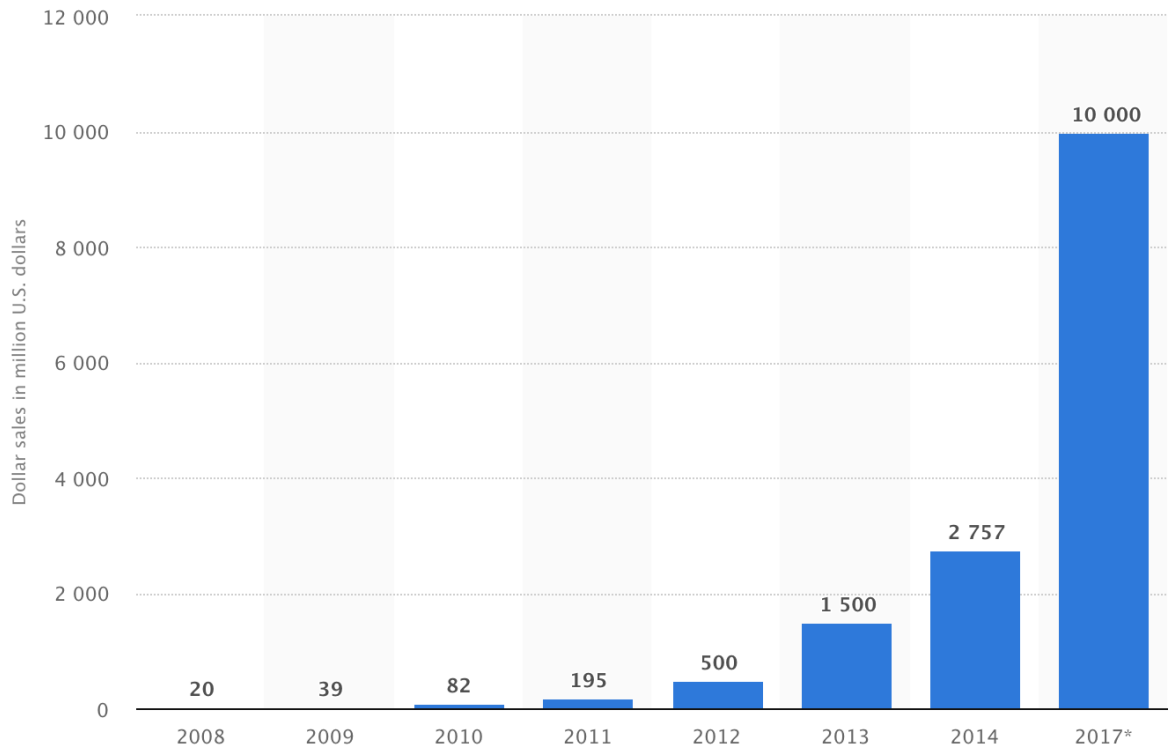
Figure 1.Electronic cigarettes (e-cigarettes) dollar sales worldwide from 2008 to 2017 (in million U.S. dollars) [2]

ECIGs have evolved through the years since their debut; there are now three generations of ECIGs available in the market. The first generation "Cig-a-like" (Fig. 2) looks like a tobacco cigarette, it comprises a disposable "Cartomizer", which hold the cartridge and the atomizer, screwed into a battery. The device is activated by a pressure sensor during inhalation, which triggers the heating element and vaporizes the liquid.
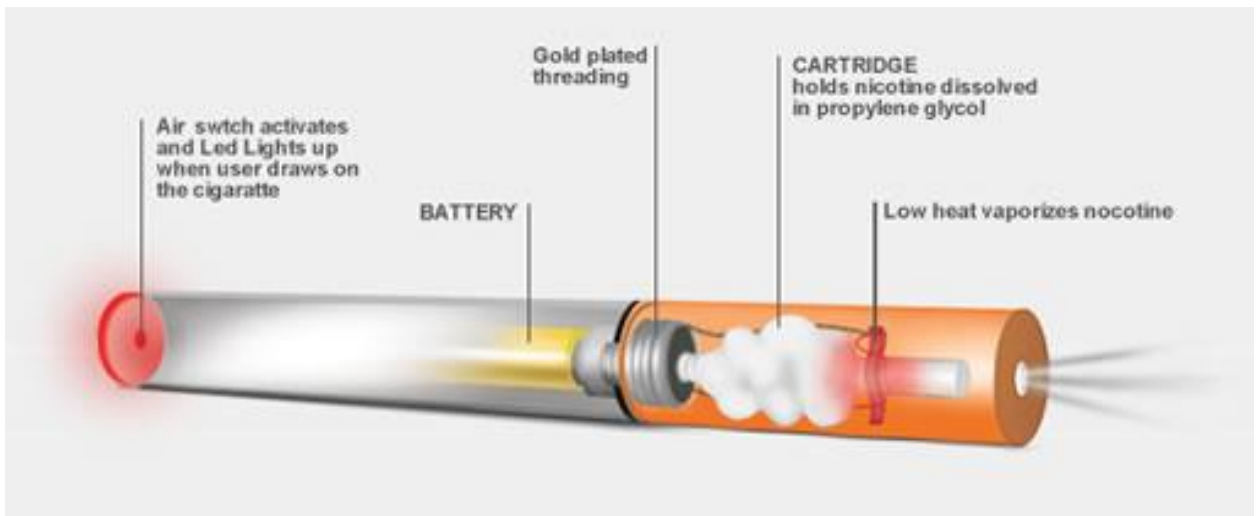
Figure 2. Schematic Diagram of first generation E-cigarette "Cig-a-like"
(http://www.pinsdaddy.com)

The second generation of ECIGs usually come with larger batteries and resembles a pen (e.g. eGo 2) (Fig.3). It consists of a refillable tank referred to as "Clearomizer" and an atomizer with a heating element that evaporates the liquid and a wicking material that draws the fluid from the tank. These devices are activated manually by a button and some may have adjustable voltage units. Similar to the second generation, the third generation ECIGs contains even larger tanks (Fig. 5) but allows more personal modifications on tanks and atomizers. For example, the user can build his/her personal atomizer with lower resistance, a low-resistance atomizer yield higher heating element temperature that generates more heat affecting the amount and quality of the aerosol.

Figure 3.Second generation Ecig "eGo 2" tank system (https://www.fda.gov)
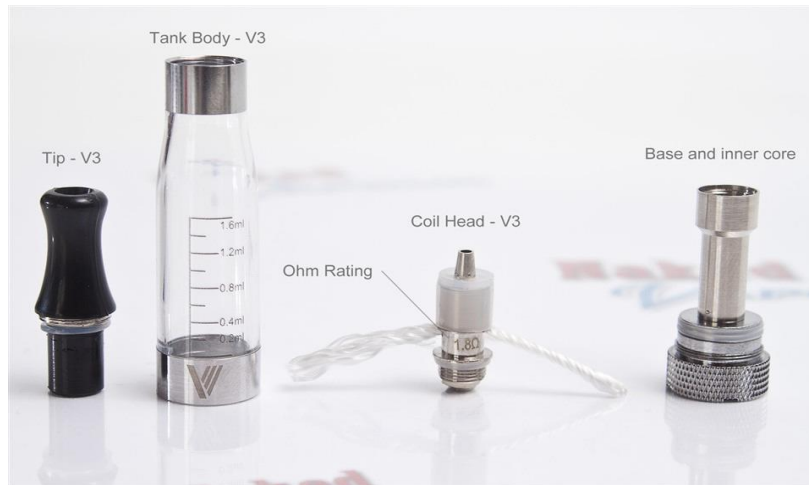
Figure 4. Tank and atomizer of "eGo 2" (https://www.nakedvapour.co.nz/search/v3-vision-ego-clearomizer)

Figure 5. Third generation Ecig (https://www.fda.gov)

ECIGs are widely available and affordable. They are typically sold in convenience and corner stores (e.g. gas stations, drug stores); suppliers are also selling them online where minors almost have complete access to buy ECIG products [7]. The Web is filled with ads and videos of ECIGs, hundreds of videos on YouTube shows people reviewing new products and liquids every day, in addition to the online ECIG forums. ECIG

companies are also endorsing celebrities and funding movies and television shows as part of their marketing strategies [8]. Several factors affected the fast spreading of ECIG devices, mainly the fact that ECIGs were completely unregulated (up until 2016) with the availability of countless models and E-liquid mixtures, and the popular belief that ECIGs are less harmful than tobacco cigarettes [9].

It has been found that there is a variation in efficacy and consistency of nicotine vaporization between different ECIG brands and models[10, 11]. Also, there is a lack of transparency on what quality standards are being applied when mixing E-liquids. In some liquids tested, investigators found variations in the chemical composition of the same flavour in different bottles [12].

Other than delivering nicotine, a psychomotor stimulant that has many side effects on the human body [10], ECIGs also deliver carbonyl compounds like formaldehyde, acetaldehyde, acetone, acrolein, propanal, croton aldehyde, butanal, glyoxal, and methylglyoxal [13]. Volatile carbonyl compounds are considered a major causative agent in pulmonary disease among cigarette smokers [14] . In addition, formaldehyde, is designated as a Group 1 carcinogen by the International Agency of Cancer [15]. Formaldehyde has been detected at high concentrations in ECIG aerosols under specific conditions [16]; Kosmider et. al [17] reported that the highest levels of carbonyls were observed in vapors generated from PG-based compared to VG-based ECIG liquid, and a 4 to more than 200 times increase in formaldehyde, acetaldehdye, and acetone levels were due to increasing the power from 4.2 to 9.6 Watts using an eGo -3 Crystal 2 clearomizer.

Formaldehyde and other carbonyl compounds formation are the result of decomposed PG when heated; it is thought that the temperature of the heating element is a critical factor in the amount of carbonyl compounds formed [18].

Due to their serious health effects, the presence of aldehydes along with other issues mentioned previously, necessitates employing regulatory actions that control the operating conditions and ECIGs designs under which these toxicants form. Key to regulation is developing the ability to predict carbonyl emissions as a function of ECIG operating and design characteristics, as has been done for nicotine emissions [19].

One main reason of aldehyde formation is known as "Dry Puff" or "Dry Hit", where the coil is overheated due to shortage of liquid supply from the wick in the atomizer. (Fig. 6) shows a top-coil tank type "clearomizer" ECIG, when the heating filament/coil is activated; the liquid inside the wick will heat up and vaporize. The hot vapor will form a "vape cloud", after its contact with fresh air drawn through the atomizer, which will eventually be inhaled by the user.
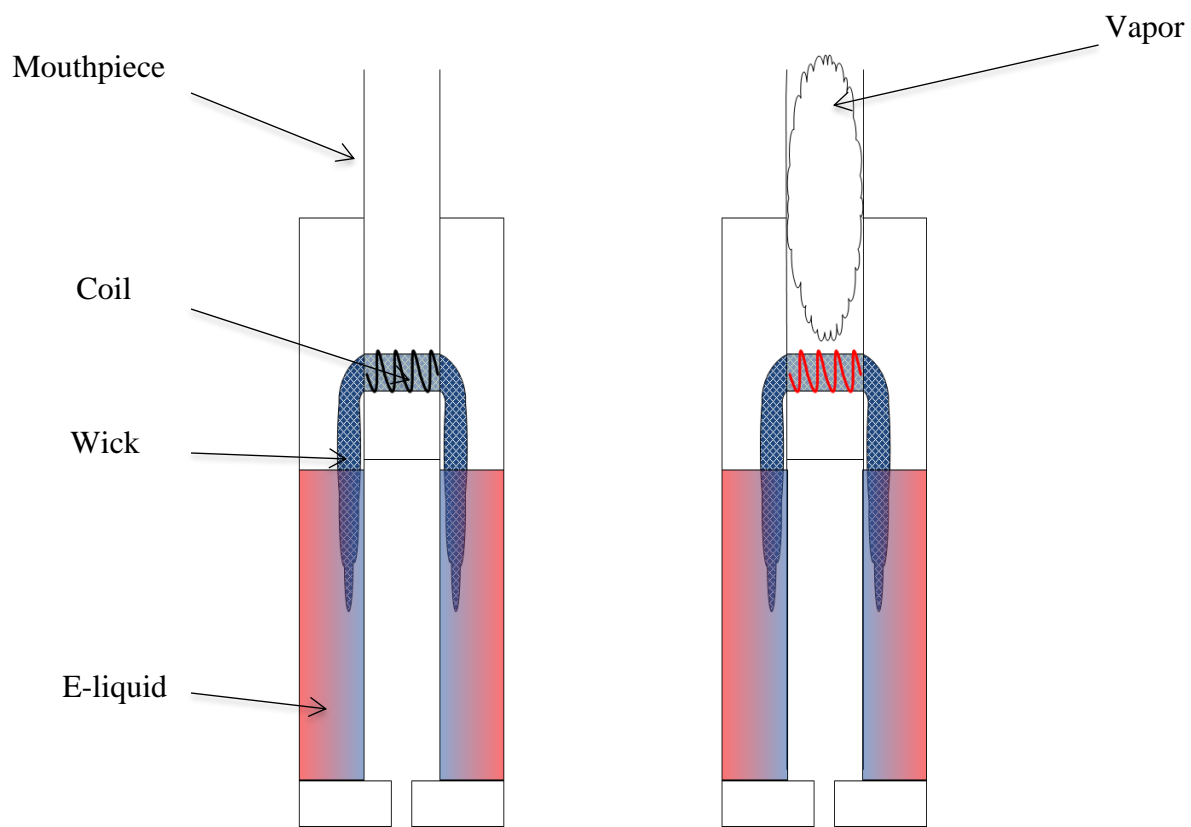
Figure 6. Ecig anatomy

The electrical energy from the battery is converted into thermal energy, which is mainly dissipated by vaporizing the liquid in the wick. Some of the thermal energy is lost by conduction to the ECIG structure and by forced convection through the fresh air drawn.

"Dry Puff" occur when the wick fail to deliver fresh liquid rapidly enough to balance the amount lost by vaporization, forming dry spots on the heating element (e.g. coil) with very high temperatures.

A. Thesis Statement

The aim of this thesis is to formulate a model that can be used to predict the liquid content inside the wick, which is directly related to a dry puff. The model must take into account the liquid and the wick properties, ECIG geometry (e.g. distance through the wick liquid must be wicked, wick diameter, heating coil dimensions), and ECIG operating conditions (e.g. puff topography, power).

By studying the properties of the wicks used and the driving force of the liquid we can predict the wicking rates and liquid content under different operating conditions, for example by varying the power, wick type, initial saturation, puff and inter-puff durations. This model will be useful for regulators and scientists to rapidly screen products for safety and efficacy with regard to emissions due to high temperature spikes from a dry puff. The innovation in this work is the application of mathematical modeling as a potential regulatory tool.

CHAPTER II

THEORY AND BACKGROUND

A. Wettability and Capillarity

In a pore space containing two fluids, one of them is attracted by the solid surface. This fluid, that has higher affinity towards solid surfaces, is called the wetting fluid/phase while the other is the non-wetting fluid/phase. In our case, the wetting phase is liquid (e.g. E-liquid) and the non-wetting phase is air. The two phases are immiscible; they are separated by an interface that is infinitely thin on a macro-scale level. This interface is characterized by a surface energy called the surface tension; it is a result of a difference in cohesion forces attracting fluid molecules on both sides of the interface. Surface tension is a measure of forces that must be overcome to change the surface shape; it creates a change in equilibrium pressures of both phases due to unbalanced tangential forces at the interface. Fig 7 shows how the presence of surface tension creates the capillary rise in small tubes.

The adhesion forces between the wetting phase molecules and the tube wall create a meniscus at the interface; the presence of cohesion force between the wetting phase molecules lifts the liquid upwards
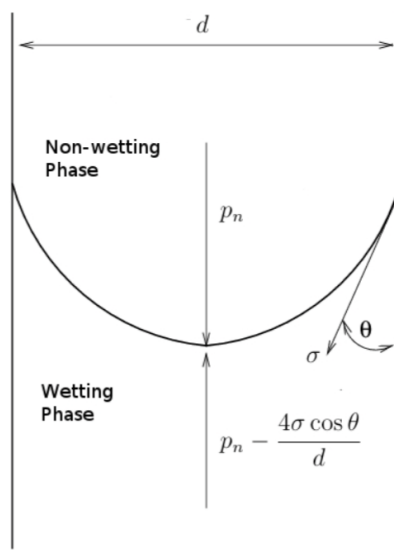
Figure 7.Capillary rise in a tube

The magnitude of the capillary force, which is the difference between wetting and non-wetting phase pressures, can be calculated using the Laplace equation:

$$\Delta p = p_c = p_{nw} - p_w = \frac{2\sigma \cos\theta}{r_c} \qquad (1)$$

Where the subscripts "nw" and "w" denotes non-wetting and wetting. σ is the surface tension, r_c is the capillary radius and θ is the contact angle between the liquid and the solid phase.

Eq. 1 shows that the capillary pressure is inversely proportional to the radius of the capillary, thus smaller radius capillaries can transport liquid to a greater heights. The flow would cease when the pressure difference become zero, that is, when the weight of the liquid present in the capillary (i.e. hydrostatic pressure) balances the capillary pressure.

1. *Wicking*

The term "wicking" means the spontaneous flow of liquid in a porous substrate driven by capillary forces, this flow is governed by liquid properties as well as the porous structure and geometry[20]. Wicking is a result of wetting in a capillary system; therefore, wicking and wetting are coupled and cannot occur in the absence of the other.

Unlike capillary tubes with given capillary radius, fibrous mediums are made up of capillaries with varying distribution of pore radii (Fig. 8). The pore structures of these mediums are complicated and very difficult to quantify. According to Dullien [21], every method of "pore size" determination defines a "pore size" in terms of a pore model which is best suited to the quantity measured in the particular experiment. Numerous assumptions are made when characterizing pore structures, the simplest possible model for capillary pressure purposes in fabrics is where the pore structure is modeled by arrays of capillary tubes usually referred to as "Bundle of Capillary tubes".

Figure 8. Microscopic structure of cotton fibre [22]

The mechanisms of capillarity dictate that liquid front moves from larger pores to smaller pores as it goes upwards. Liquid initially fills all the pores, but can travel only to certain heights in the larger pores where it then migrates to the smaller pores (i.e. higher capillary pressure), and so as the height of the liquid front increases, the liquid content inside the sample decreases because not all pores are being filled.

2. Capillary pressure function.

As mentioned above, capillary pressure in a porous medium is a function of wetting and non-wetting phase saturations, where the saturation of the phase i is defined as:

$$S_i = \frac{Volume\ of\ phase\ i\ in\ sample}{Total\ pore\ volume\ of\ the\ sample} \qquad i = w, nw \qquad (2)$$

For example, in a water-air system, If the medium is initially fully saturated by water (e.g. the wetting phase), it can be invaded by the air phase if the gas pressure exceeds the water pressure by a specific value, the corresponding value is called "breakthrough" or "entry" capillary pressure [23]. At this point, water saturation decreases with the increasing value of the capillary potential. Saturation levels of the liquid phase is also an important parameter for determining the permeability, as will be discussed later on.
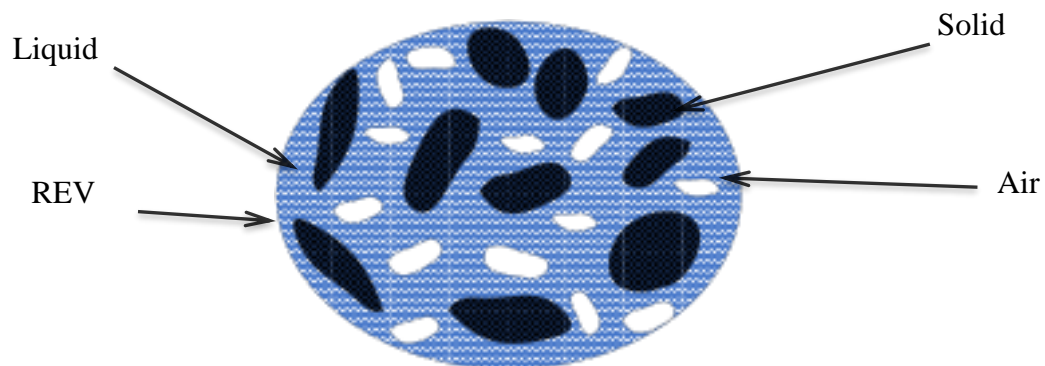
Figure 9.Pore-scale representative elementary volume (REV)

B. Macroscopic Description Of Flow

Flow through porous mediums is largely dependent on the scale considered [24]. At small scales, if one looks at one or two channels, it is possible to use conventional fluid mechanics to describe the flow. However, when a larger scale is considered, where many channels are involved, the complexity of flow paths rules out the conventional approach.

Therefore, a volume averaging approach is used where the relevant physical quantities defined at a given point **x** represent averages taken over a pore-scale representative elementary volume (REV) associated with that point (Fig. 9).

1. *Darcy's Law and Permeability*

Darcy's law has been used to describe the motion of liquid through porous materials. Henry Darcy (1856) observed that the flow rate of water through beds of sand is proportional to the loss of pressure. Darcy's law is empirical; it is derived from experimental observations. Darcy's law for fluid flow in the pore space is given by the relationship

$$Q = \frac{AK}{L}\Delta h \tag{3}$$

Where Q (m^3/s) is the volumetric flow rate, A (m^2) is the cross sectional area perpendicular to the flow, L (m) is the length of the sample in the macroscopic flow direction, K (cm/s) is the hydraulic conductivity and h (m) is the hydraulic head. Darcy's equation shows that the flow rate is directly proportional to the head difference; the coefficient of proportionality is the hydraulic conductivity K, it is a linear law similar to Ohm's law of electricity and Fourier's law of heat conduction. The hydraulic conductivity K here is a function of fluid properties and pore geometry. Darcy's equation can be written in terms of the pressure head as

$$Q = \frac{Ak}{\mu}(\frac{\Delta P}{L}) \tag{4}$$

14

k (m^2) is now the permeability of the medium at full liquid saturation, it is an intrinsic property of the porous material and it's only a function of the solid matrix. The intrinsic (or absolute) permeability k of a porous material represents its ability to allow the fluid to flow through. k is a tensor that can be same or different in different directions, depending on whether the porous matrix is isotropic or anisotropic. Eq. 4 has been found to be applicable for Reynolds number of up to unity (e.g. creeping flows)[25]. In a more general case of three-dimensional single-phase fluid flow in a medium characterized by arbitrary pore geometry and adding the gravitational effect yields the following equation [26, 27]:

$$Q = -\frac{kA}{\mu}(\nabla p - \rho g) \tag{5}$$

2. Unsaturated Porous Medium and Permeability Function

In the discussion above (section a), Darcy's equation represent flow in a fully saturated porous medium, which means that the pore space is filled with a single fluid. Now we will discuss flow of fluid in a porous medium with air pockets filling part of the pores, such mediums are said to be "unsaturated". We previously defined the term "saturation" (Eq. 2); liquid saturation represents the fraction of pore space filled with liquid phase.
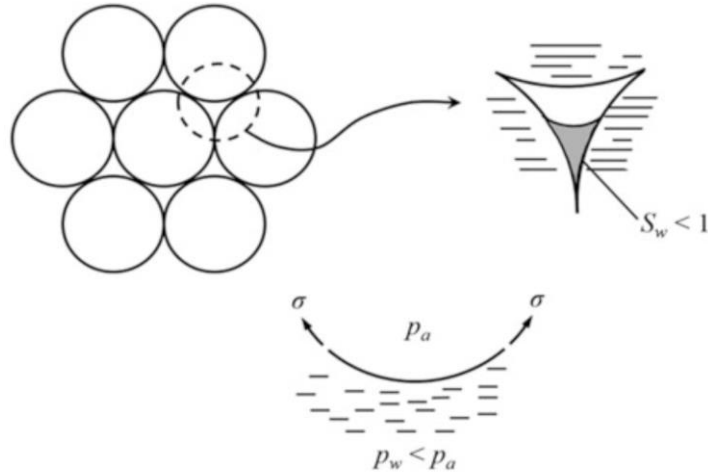
Figure 10.Formation of liquid-air interfacial forces in unsaturated porous media [28]

Interfacial forces are present in an unsaturated porous medium. In a liquid-air system, a meniscus will form within the pore space (Fig. 10) where under equilibrium conditions; pressure of the liquid phase is smaller than that of the air phase [28]. If the subject of interest is the flow rate of the liquid and how fast it is saturating the medium, it can be assumed that the pressure of the gas (e.g. air) phase equals the atmospheric pressure. The flow in our case is driven by the capillary pressure when it exceeds the force of surface tension at the interface.

The extended form of Darcy's equation that includes the relative permeability function in unsaturated mediums for each phase was first introduced by Muskat and coworkers [29] and is written as:

$$Q_i = -\frac{k_i A}{\mu_i}(\nabla p_i - \rho g) \qquad i \tag{6}$$

$$= w, nw$$

Where k_i is referred to as "effective permeability" or "phase permeability" of the porous medium to fluid i [21] and it is a function of the phase saturation.

It is also customary to introduce the relative permeability term "k_{ri}" where

$$k_{ri} = \frac{k_i}{k} \tag{7}$$

k is the absolute permeability from eq. 5. k_{ri} ranges from 0 to 1 where $k_{ri} = 1$ corresponds to a medium fully saturated with phase i.

The phase permeability decreases with decreasing liquid saturation (S_w), since the presence of air steepens the interface curvature and creates more resistance on the flow, while a higher saturation with more liquid filling the pores increases the permeability.

If we are interested in a liquid-air system, the velocity of each phase can be presented as:

$$v_l = -\frac{k_l}{\mu_l}(\nabla p_l - \rho g) \tag{8}$$

$$v_a = -\frac{k_a}{\mu_a}(\nabla p_a - \rho g) \tag{9}$$

The non-wetting phase being air, it can be assumed that its pressure equals atmospheric pressure ($P_a = P_{atm}$) leading to zero velocity in the non-wetting phase, and neglecting the effect of gravity, leaves us with only one momentum equation:

$$q_l = -\frac{k_l}{\mu_l}(\nabla p_w) \tag{10}$$

For simplification, in the coming sections, liquid saturation will be referred as "S" and permeability as "k".

C. Model Formulation

During a puff, the coil is powered and air is drawn through the ECIG over the coil-wick unit (Fig. 11) to vaporize the e-liquid. As the formed hot vapor mixes with fresh air, it re-condenses again forming an aerosol mist that will eventually be inhaled by the user. The wick acts as a medium to transport fresh liquid from the tank to the heating element. From the above description, two main processes are happening during a puff: evaporation and wicking (Fig. 11).

In this work, the effort is focused on developing a model to predict the flow rate of e-liquid in the wick. A similar model was originally developed by Talih et al [1] that predicts nicotine emissions in ECIGs without addressing the wicking behavior, where it was assumed that the wick is always fully saturated with liquid. The current model follows the same procedure in solving conservation equations, however it includes the effects of wicking. The model requires inputs to give predicted outputs; these processes will be more elaborated upon in the subsequent sections.
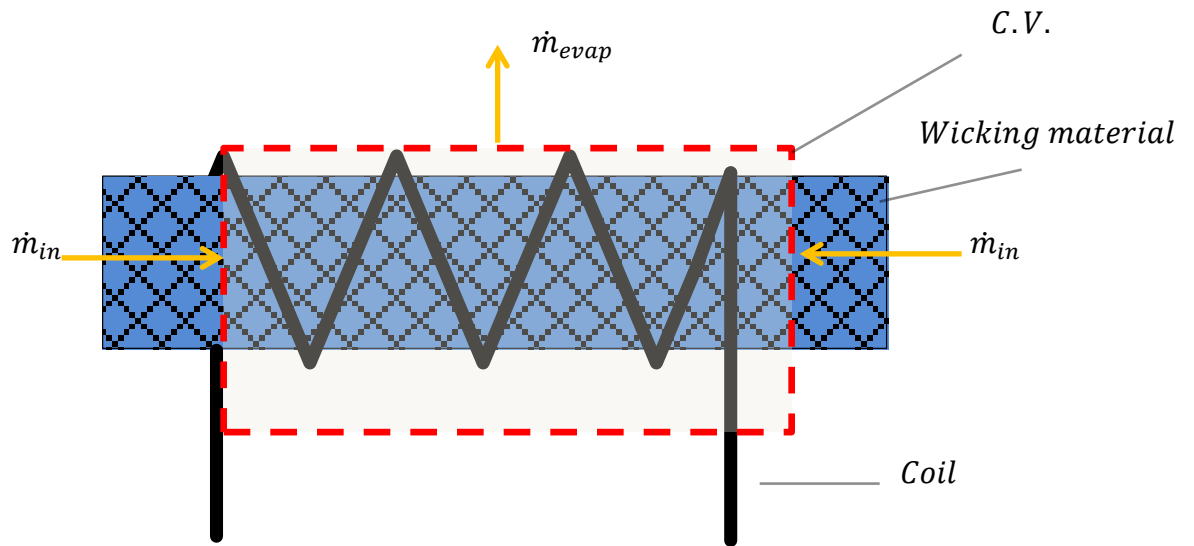
Figure 11.Coil-wick unit CV (dashed line) with mass fluxes shown.

As discussed above, two fundamental properties used to predict the overall wicking rate, capillary pressure and permeability which are in turn dependent on the liquid saturation (S) present in the wick; therefore, to predict $\dot{m}_{in}$, $\dot{m}_{evap}$ must first be known. Permeability and capillary pressure are coupled in Darcy's equation (e.g. momentum equation).

Energy and mass conservation equations are the main equations used in this model in order to compute $\dot{m}_{in}$ and $\dot{m}_{evap}$. The control volume in figure 11 is divided into two equal parts, since both ends of the wick are dipped in fresh liquid from the tank forming a symmetry boundary condition at the center (Fig. 12).
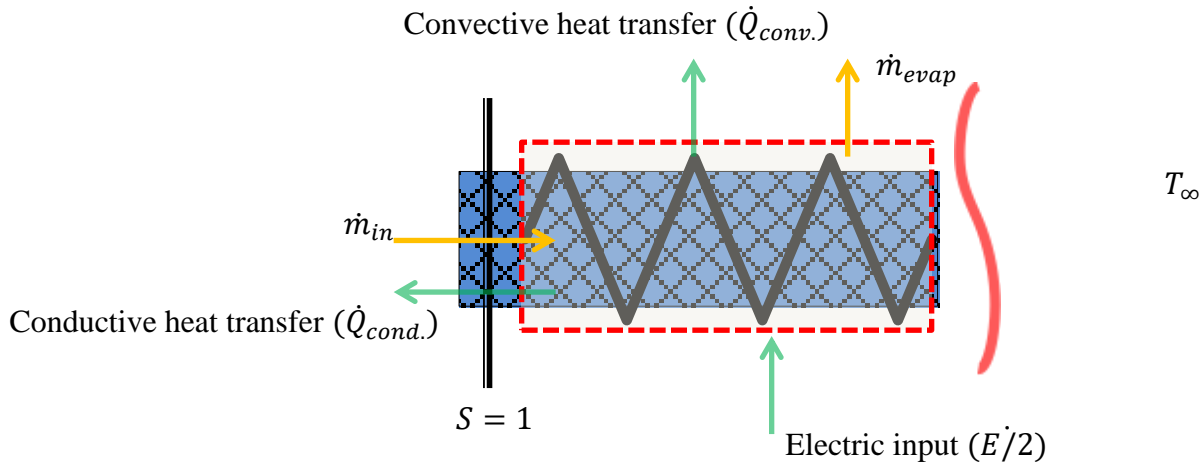
Figure 12.New CV with heat and mass fluxes.

1. *Single Zone Control Volume Model*

In the simplified model, the control volume is taken as a single zone where all the properties are evaluated assuming the saturation level is uniform along the CV. There are several challenges to model flow in porous medium. For example, the structure of the saturated porous medium consists of a solid matrix, e-liquid and air making it difficult to predict the heat and mass transfer of the medium. Also, transport properties have a non-linear relationship with temperature and saturation levels. Fiber swelling may affect the porosity significantly, varying the available void space for liquid and air. To simplify the problem, several assumptions are [30]:

- The fibrous system is represented by an ideal continuum medium and is divided into volume fractions of liquid, solid and air at a particular location. The inhomogeneity scale of the three-phase, solid, liquid and gas system is far

smaller than the characteristic length over which an appreciable change in moisture content occurs.

- The solid phase is considered to be non-deformable. Based on this assumption, mechanical swelling and shrinkage of the solid phase are not included. Some fibers, particularly natural materials, do swell. However, in actual fabrics the fiber is usually a small portion of the total volume. Therefore, any swelling that may occur has a relatively small effect on the void space for moisture movement. Also, experimental data for permeability will reflect the effects of swelling.

- Darcy's equation is used to describe the transient flow through the saturated and unsaturated regions in the fibrous medium, since the liquid is flowing at a very low Reynolds number.

- The liquid component is incompressible.

The energy conservation equation is employed to compute the instantaneous temperature of the CV. Figure 12 shows the thermal energy flows where the input electrical power is converted into thermal energy. The thermal energy is dissipated as heat lost to the air flowing over a cylinder, heating and vaporization of liquid in the CV, heat lost by conduction to the surroundings through the wick and liquid and the heating up of the CV itself. The integrated form of the unsteady energy equation to compute the instantaneous temperature T (K) of the CV is written as:

$$C \, \frac{dT}{dt} = \dot{E} + (\dot{Q}_{cond.} + \dot{Q}_{conv.} + \dot{Q}_{lat.} \qquad (11)$$
$$+ \, \dot{Q}_{liq.})$$

$\dot{E}$ is the electrical power input in Watts and:

$$C = (1 - \epsilon)V_{CV}\rho_s C_{p,s} + S\epsilon V_{CV}\rho_{liq}C_{p,liq.} \tag{12}$$

C is the effective heat capacity of the liquid-wick system, where ϵ is the porosity

of the wick (dimensionless), V_{CV} is the volume of the CV (m^3), ρ is the density ($\frac{kg}{m^3}$), S is

the liquid saturation, C_p is the specific heat $\left(\frac{J}{kg.K}\right)$. The subscripts "$s$" and "$liq$" represent

solid matrix and liquid.

$$\dot{Q}_{cond.} = K_{cond.}A_{CS}(T - T_\infty) \tag{13}$$

$\dot{Q}_{cond.}$ is the rate of heat transfer by conduction through the wick (W),

$K_{cond.}$ ($\frac{W}{m.K}$) is the effective thermal conductivity of the liquid-fiber combination and can

be written as:

$$K_{cond.} = (1 - \epsilon)K_s + S\epsilon K_{liq.} \tag{14}$$

K_s and $K_{liq.}$ Are the conductivities of the solid matrix and liquid respectively. A_{CS}

is the cross-sectional area of the CV (m^2).

$$\dot{Q}_{conv.} = hA_S(T - T_\infty) \tag{15}$$

$\dot{Q}_{conv.}$ Is the rate of heat transfer by convection to the fresh air flowing over a

cylinder (e.g. CV) (W). h is the convective heat transfer coefficient and is estimated

assuming cross flow over a cylinder $\left(\frac{W}{m^2 K}\right)$. A_S is the surface area of the CV (m^2).

$$\dot{Q}_{lat.} = \dot{m}_{evap.}h_{fg,liq} \tag{16}$$

$\dot{Q}_{lat.}$ is the latent heat associated with change of phase from liquid to vapor, $\dot{m}_{evap.}$

Is the liquid vaporization rate $\left(\frac{Kg}{s}\right)$ and $h_{fg,liq}$ is the latent heat of vaporization $\left(\frac{J}{Kg}\right)$.

$$\dot{Q}_{liq.} = \dot{m}_{in} c_{p,liq} (T - T_\infty) \tag{17}$$

$\dot{Q}_{liq.}$ is the energy expended heating the fresh liquid entering the CV from the

tank, $c_{p,liq}$ is the specific heat of the liquid $\left(\frac{J}{kg.K}\right)$.

Two regimes control the vaporization process, evaporation and boiling. When the

instantaneous temperature T of the CV is below boiling (T_b), $\dot{m}_{evap.}$ is computed assuming

convective mass transfer:

$$\dot{m}_{evap.} = h_m \, A_s \frac{M_{liq.} P_v}{Ru.T} \tag{18}$$

h_m is the mass transfer coefficient $(\frac{m^2}{s})$, $M_{liq.}$ is the molar mass of the evaporating

liquid $(\frac{Kg}{mol})$, Ru is the universal gas constant $\left(\frac{J}{mol.K}\right)$ and P_v is the vapor pressure of the

evaporating species computed at T using Antoine equation (Appendix A).

If the instantaneous temperature of the CV reaches the boiling temperature of the

liquid (T_b), the boiling regime prevails where the temperature of the CV is maintained

constant at T_b and $\dot{m}_{evap.}$ is calculated by balancing Eq. 11:

$$\dot{m}_{evap.} = \frac{\dot{E} + (\dot{Q}_{cond.} + \dot{Q}_{conv.} + \dot{Q}_{liq.})}{h_{fg,liq}} \tag{19}$$

It is assumed that the wick is initially fully saturated (e.g. all the pores are filled

with liquid). During a puff, after $\dot{m}_{evap.}$is computed during both regimes, $\dot{m}_{in}$ can be

estimated by using Eq. 9 where the values of k_l and p_w are function of liquid saturation in

the CV.

As mentioned previously, the model requires inputs to get predicted outputs. The

inputs of the

model are the following:

- Puff topography (puff duration, inter-puff interval)

- Electrical power input

- Heater element dimensions (e.g. diameter and length)

- Wick dimensions and porosity

- Thermodynamic and transport kinetic properties of e-liquid (Appendix A).

    The user can vary all of the inputs, except for the e-liquid properties.

    The outputs of the model are:

- Saturation levels in the CV

- Temperature of e-liquid

- $\dot{m}_{evap}$

- $\dot{m}_{in}$

2. *Multi-CVs Model*

The non-uniform heating of the coil during a puff creates an uneven temperature distribution within the CV with sections having higher temperatures than others; therefore, to track aldehyde formation more accurately along the CV, the single-zone CV is further divided into smaller CVs (Fig. 13) .
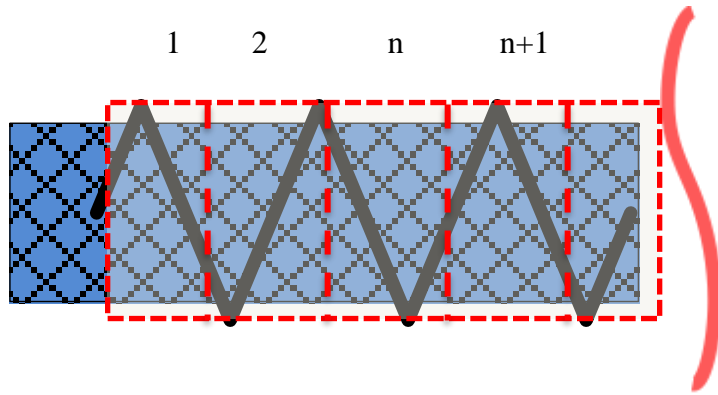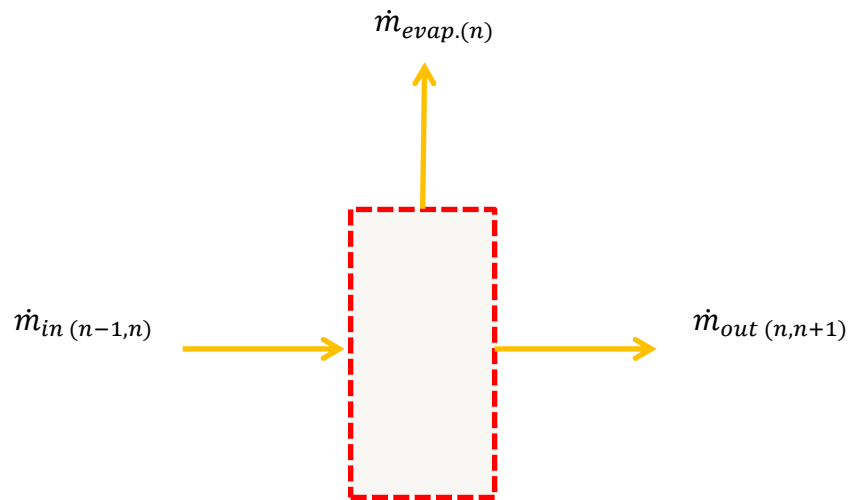
Figure 13.Multiple CVs.

Figure 14.Single CV with mass fluxes.

Figure 14 shows what is happening at the boundary layer of every CV with $S = 1$ at the boundary of the first CV (Fig. 12), and $\dot{m}_{out} = 0$ for the last CV since it is a symmetric boundary. Same principles discussed above for a single zone CV applies here to get the mass flowing in, out and evaporated for each CV. The number of CVs is added to the model as an input to compute the electrical power input at each CV by dividing the total input over the number of CVs.

CHAPTER III

MATERIALS AND METHODS

A. Wick and Liquid Selection:

There are many kinds of wicks available for use in ECIGs including Ekowool™, cotton, cellucotton rayon fibers, stainless steel mesh and others (Fig. 15). The choice depends entirely on the user, though the early type of ECIGS (e.g. Clearomizers) came with a standard silica wick.

(a)

(b)

(c)

(d)

Figure 15.(a) Cotton (b) Cellucotton rayon fibers (c) Stainless steel mesh (e) Ekowool™ (http://www.drapervapor.com/10-types-vape-wicks/)

Ekowool™ (Fig. 16) was used in the experimental setup for several reasons, mainly for its ease of use and producing consistent results. For example, it is much easier to cut a specified length of Ekowool wick than cotton; this is a decisive parameter for the experiment to produce clean, repeatable results. Ekowool™ wicks are braided silica fibers (Fig. 17) made from silicon dioxide (SiO_2) designed originally for use in a high temperature environment and heat insulation, it have low thermal conductivity, high resistance to thermal shock at high temperatures. According to the manufacturer, Ekowool™ can also be used for long periods of time at temperatures up to 1000°C without changing its properties. These factors made Ekowool™ popular and favorable to ECIG users.
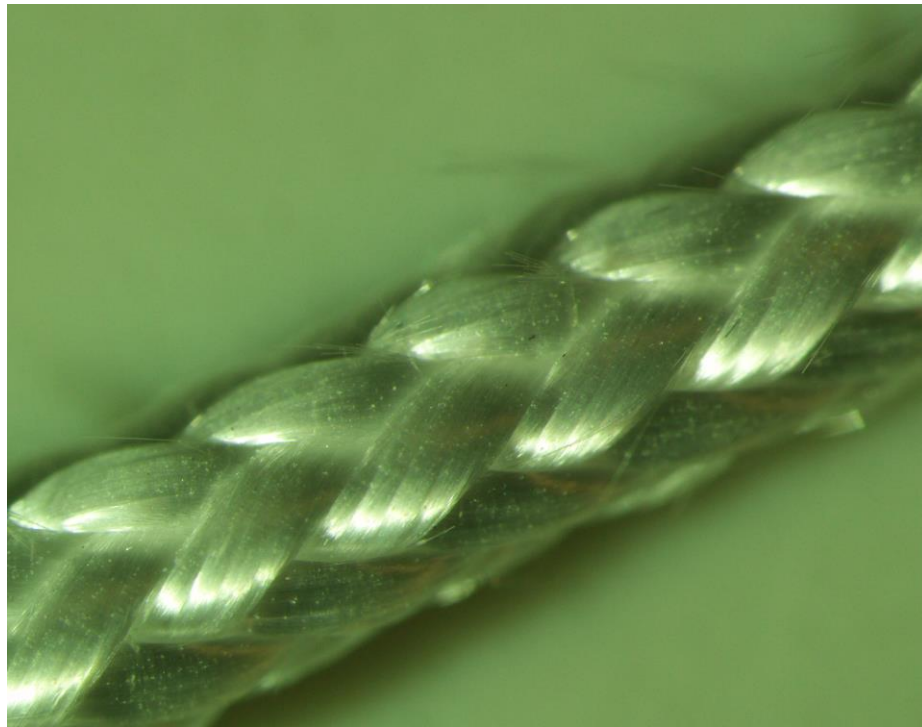

Figure 16.Ekowool™ wick

Figure 17.Silica fiber from Ekowool™

As for the e-liquid, PG was used since it is more prevalent than VG-based liquids. However, with the rising popularity of sub-Ohm (<1 Ohm) devices, VG liquids have been gaining popularity [31].

B. Setups and Procedures:

1. Capillary Pressure vs. Saturation.

As mentioned before, we need to find the relation between the liquid driving force, which is the capillary pressure (P_c), and saturation levels (S) inside the wick. For this purpose, the "long column" method was performed on our samples [32], this method was

originally used to measure the capillary pressure of unconsolidated materials that can be packed into a long column (e.g. sand, clay); however, the principle behind this method is the same and it is analogous to a capillary tube pulling water from a reservoir, where the differential pressure at the interface between water and air is equal to the capillary pressure. The fluid wicks to a height at which the capillary pulling force is balanced by the weight of the fluid column, at this point the liquid front cease to advance and equilibrium is reached. In fabrics, there is a distribution of pores and the fluid will be wicked to varying heights depending on the diameter of the capillary, this relation is described by the Laplace equation (Eq.) which shows that smaller capillaries lifts the fluid higher, where γ is the fluid surface tension and θ is the wetting angle. Consequently, the saturation decreases as liquid moves vertically upward.

$$P_c = \frac{2\gamma \cos \theta}{R} \hspace{4cm} (20)$$

Measuring saturation at different vertical locations of the sample enables us to determine capillary pressure as a function of saturation. A 70 cm long ekowool wick samples, with 2 cm diameter were cut and suspended above a reservoir that held propylene glycol (PG) (Fig. 18). A small weight was attached to the submerged part of the wick to keep it straight and prevent it from curling during the experiment. The samples were previously marked with a water-proof pen (Fig.) to indicate where they would be cut at the end of the experiment. The specimen also was covered with a glass tube during the experiment to minimize evaporation losses to air due to mass transfer.
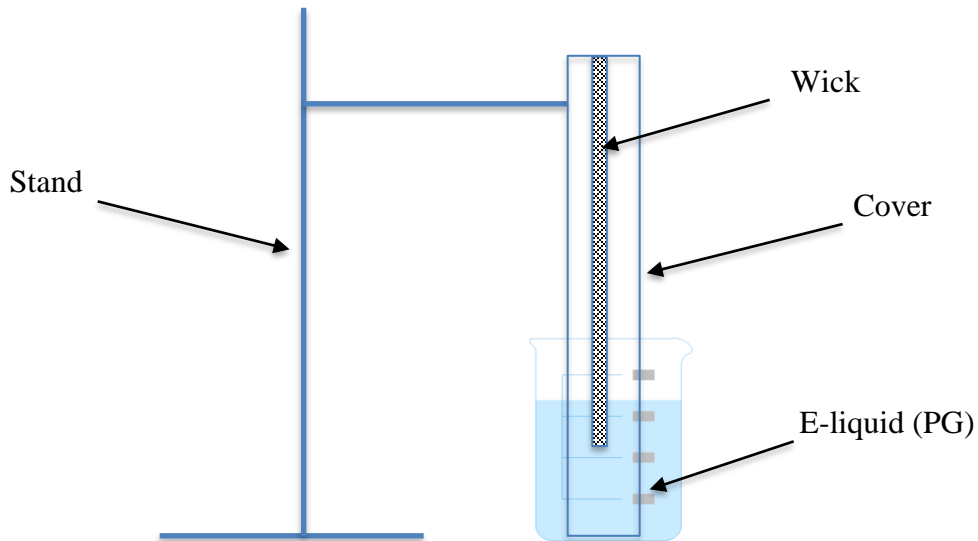
Figure 18."Long column" setup

The samples were left for 24 hours to establish equilibrium (e.g. liquid front stops), then each specimen was cut into small sections 2cm in length, these pieces were directly weighed after cutting then moved to an oven to accelerate the drying process, the oven's temperature was maintained at 65°C. From both measurements saturation can be calculated by:

$$S = \frac{(m_w - m_d)/\rho_{PG}}{\epsilon V_T} \tag{21}$$

where m_w and m_d are the wet and dry weights of the sample respectively (Kg), ρ_{PG} $(\frac{Kg}{m^3})$ the density of PG and V_T (cm^3) is the total volume of the specimen piece.

2. *Permeability vs Saturation.*

Since there is no commercially available test apparatus or a universal standard method for finding the effective permeability "k_l" (Eq.7) of fibrous materials, a suitable

30

apparatus had to be designed and constructed. The setup consists of two analytical balances (Fig. 20), a coil-wick unit attached to the hook of Balance 1, while the wick ends are dipped in a beaker filled with E-liquid (PG) placed on Balance 2 (Fig. 20), both balances are connected to a PC with an RS-232 (serial) cable. The power is controlled and delivered to the coil using an external power supply and a "DNA 200" board (Fig. 19), this board is a DC-DC converter used in ECIGs to control power and measure different parameters (e.g. Coil resistance, Voltage etc..). A LabVIEW code was responsible to collect the data from the balances and communicate with the board to control the power and enable the user to select puff and inter-puff durations; the balances can also be zeroed using the software.

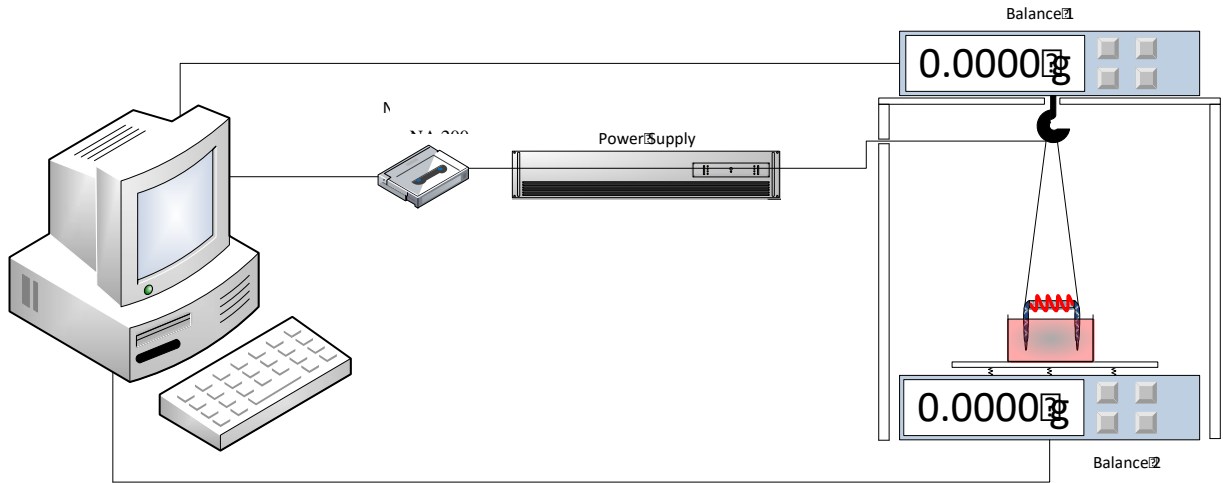Figure 19.DNA 200 board (https://www.evolvapor.com/products/dna200)

Figure 20.Experimental setup to get permeability "k"

After suspending the coil-wick unit, the wick ends are submerged in the liquid and wicking starts immediately, the readings of the balances start changing accordingly.

When equilibrium is reached (e.g. the readings of the balances are not changing) the balances are zeroed and the coil is powered to start the vaporization process (e.g. puffing) causing a perturbation of the steady state and triggering wicking again due to a saturation gradient. The puff duration should be long enough for the system to reach steady state, where $\dot{m}_{in} = \dot{m}_{evap}$, at this point the saturation (S) in the control volume is maintained constant so that at any given saturation, $\dot{m}_{in}$ (e.g. wicking rate) can be estimated and used in Darcy's equation (Eq.) along with the previously established P_c-S relation to get the permeability (k_l) as a function of saturation. Figure 21 shows a sample of the collected data.
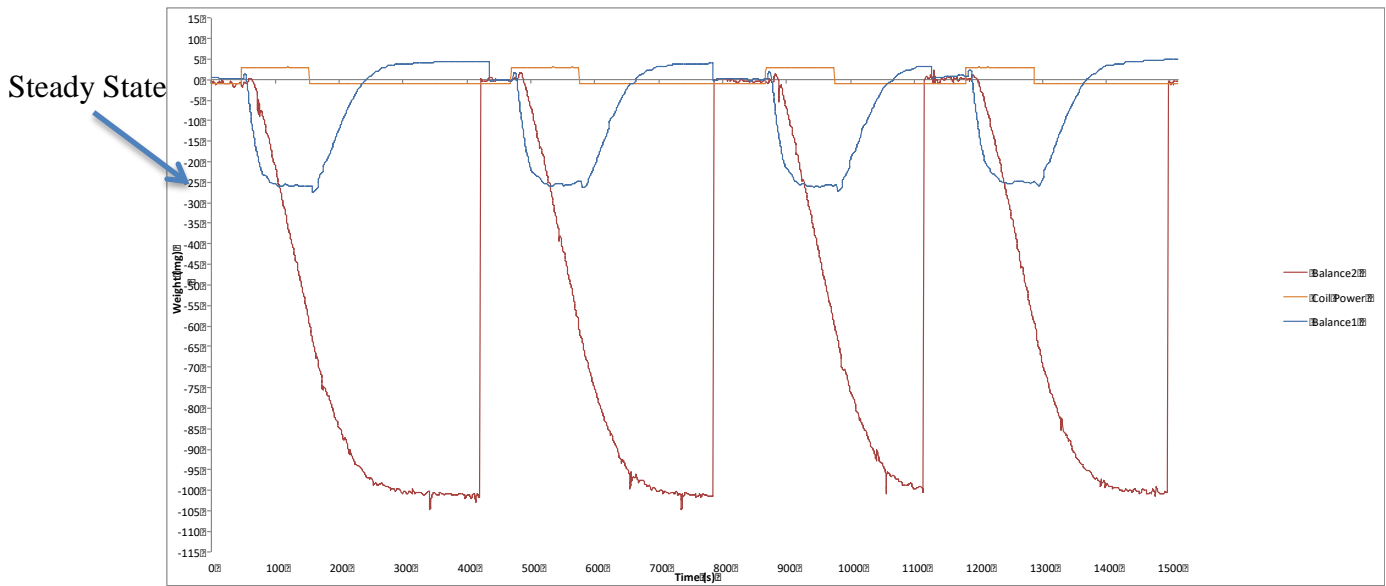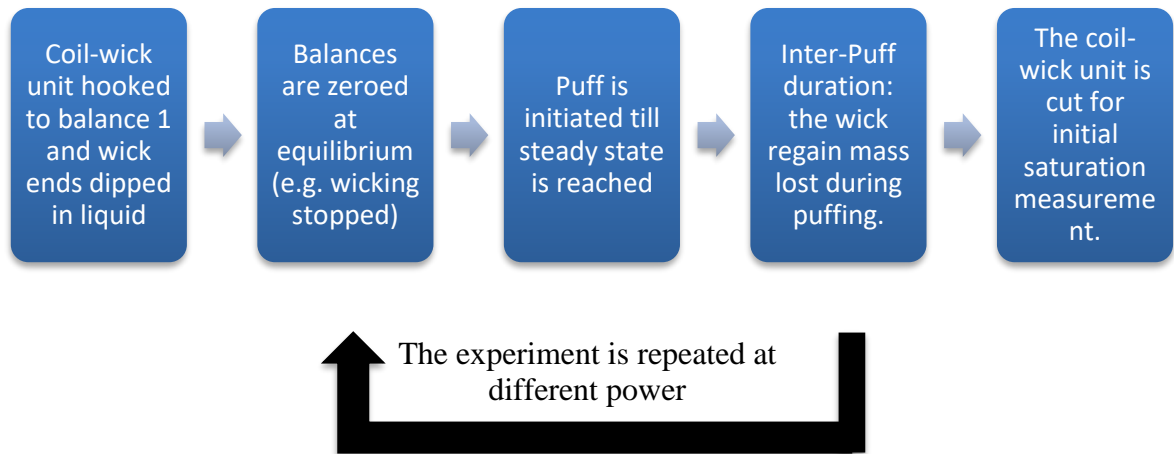
Steady State

Figure 21.Sample of data collected (3 Watts, 80-s puff)

The readings from both balances (mg) are plotted vs time (s) (Fig. 21). During a puff, the reading of balance 1 holding the coil-wick unit starts decreasing until steady state is attained where $\dot{m}_{in} = \dot{m}_{evap}$; at this point, the reading of Balance 1 becomes constant and $\dot{m}_{in}$ is calculated from the slope of Balance 2 readings during steady state interval.

The saturation (S) is determined by the weight lost at steady state where the initial saturation is determined at the end of the experiment by cutting the CV when its in the equilibrium state and getting its dry and wet weights (Eq.). For example, if the wick can hold 40 mg of e-liquid to reach full saturation (e.g. $S = 1$) and it loses 20 mg at steady state, the saturation level at steady state would be 50%. It can be noticed from figure 21 that at the end of the inter-puff duration, the coil-wick unit gains more mass (e.g. Balance 1 reads value > 0 mg) this is an experimental error and it's due to vapor condensation on the hook; therefore both balances are zeroed again before starting another puff. The whole

33

process is repeated at different power ratings to get different saturation levels at steady

state. Reproducibility of test results can be found in Appendix B. The chart below explains

the steps discussed above:

| Coil-wick unit hooked to balance 1 and wick ends dipped in liquid | → | Balances are zeroed at equilibrium (e.g. wicking stopped) | → | Puff is initiated till steady state is reached | → | Inter-Puff duration: the wick regain mass lost during puffing. | → | The coil-wick unit is cut for initial saturation measurement. |

The experiment is repeated at different power

CHAPTER IV

RESULTS

A. Capillary Pressure (P_c) vs. Saturation (S)

Fig. 22 shows the results of saturation (%) vs. capillary pressure (Pa) from three different samples using the "long column" test. Due to the experimental procedure, which requires hand cutting of the samples, and also the variability of the wicking material itself, values obtained are not expected to be exactly the same, but are expected to fall within an accepted spread of values.
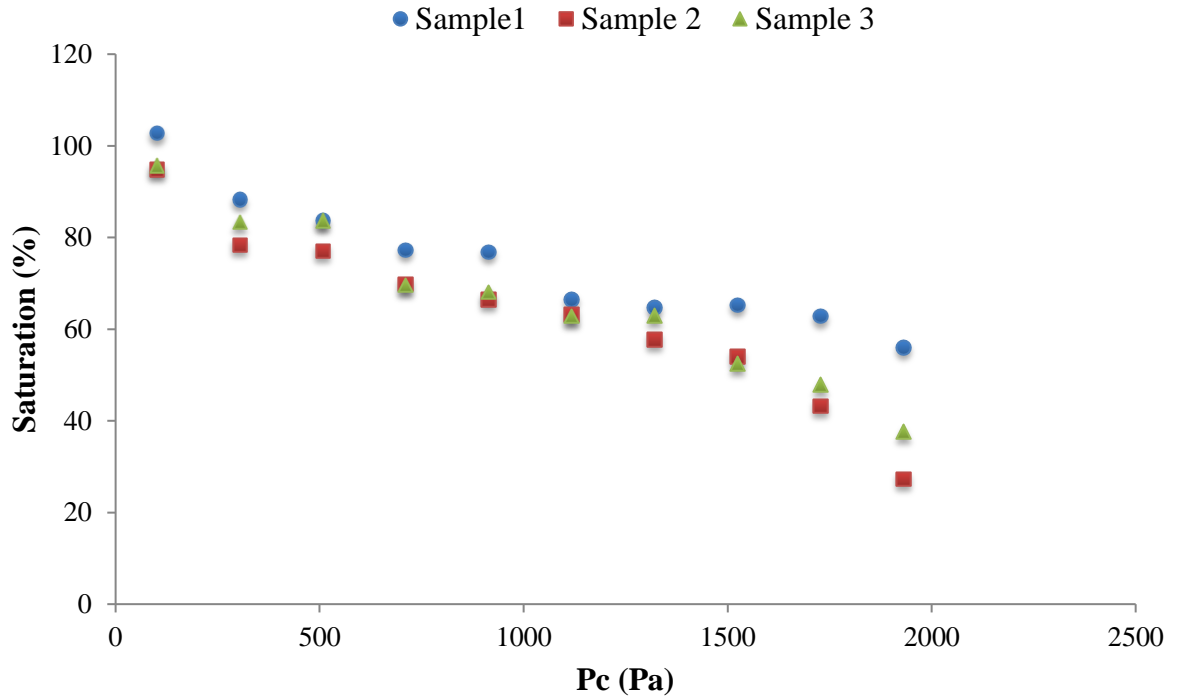

Figure 22.Capillary pressure vs. saturation for three different samples.

As explained earlier, preparation of the samples becomes increasingly important when talking about reproducibility. If the samples are not accurately cut, the data may be misleading.

The readings of the three samples are averaged and plotted vs. saturation fraction (dimensionless) (Fig. 23). The equation of the best-fit line as well as the R^2 value is also given in the figure.
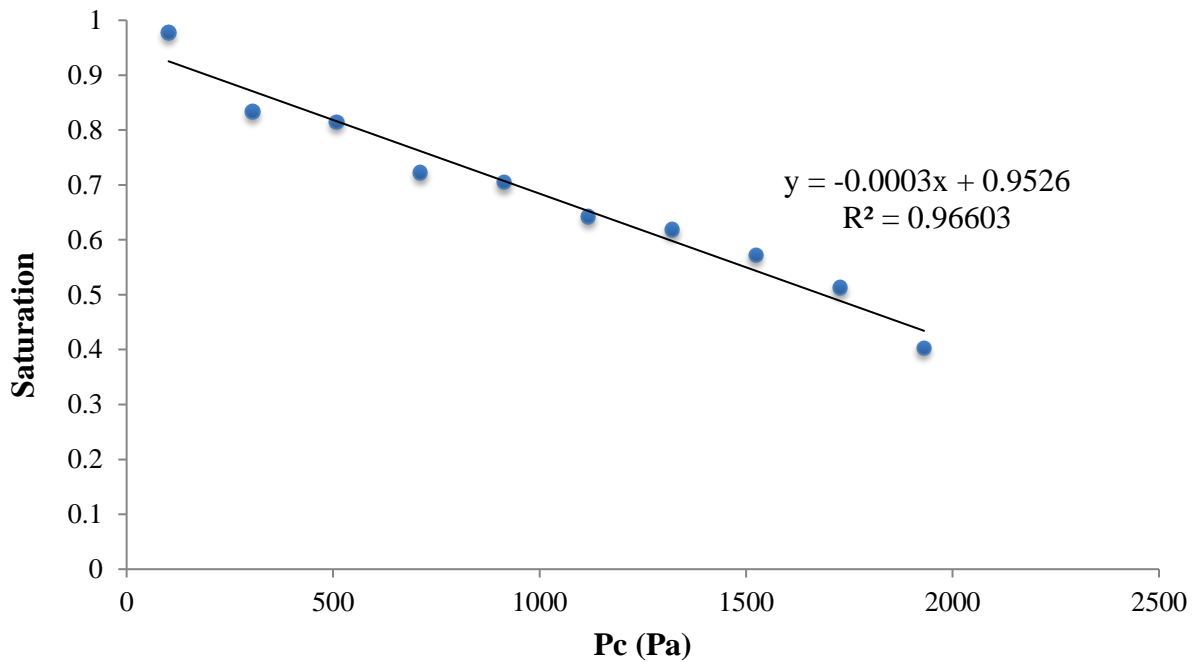

Figure 23.Capillary pressure vs. saturation

The best-fit line seems to offer a reasonable linear relationship with an R^2 value of 0.96. The equation in Fig. 23 represents the $P_c - S$ relation which will be plugged in the model.

B. Permeability (k) vs. Saturation (S)

The permeability (k) can now be calculated using Eq. 9 with all other variables now computed. Fig. 24 shows the results of Q_{in} vs. S for three different experimental conditions where the number of coil wraps around the wick was changed to check if it affects the wicking phenomena. Q_{in} is computed from $\dot{m}_{in}$ data.
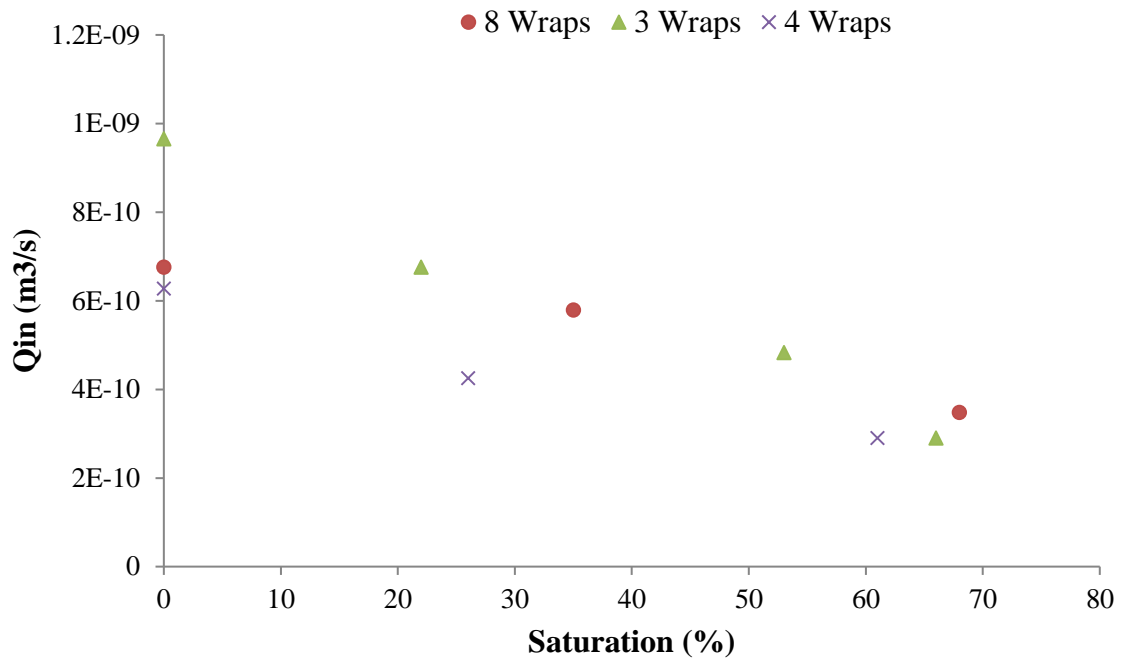

Figure 24. $\boldsymbol{Q_{in}}$ vs. saturation

The results of the three different experiments seem to agree with a slight variation. The $k - S$ relation can be computed by averaging the readings of figure 24 and substituting in Eq.9 (Fig. 25).
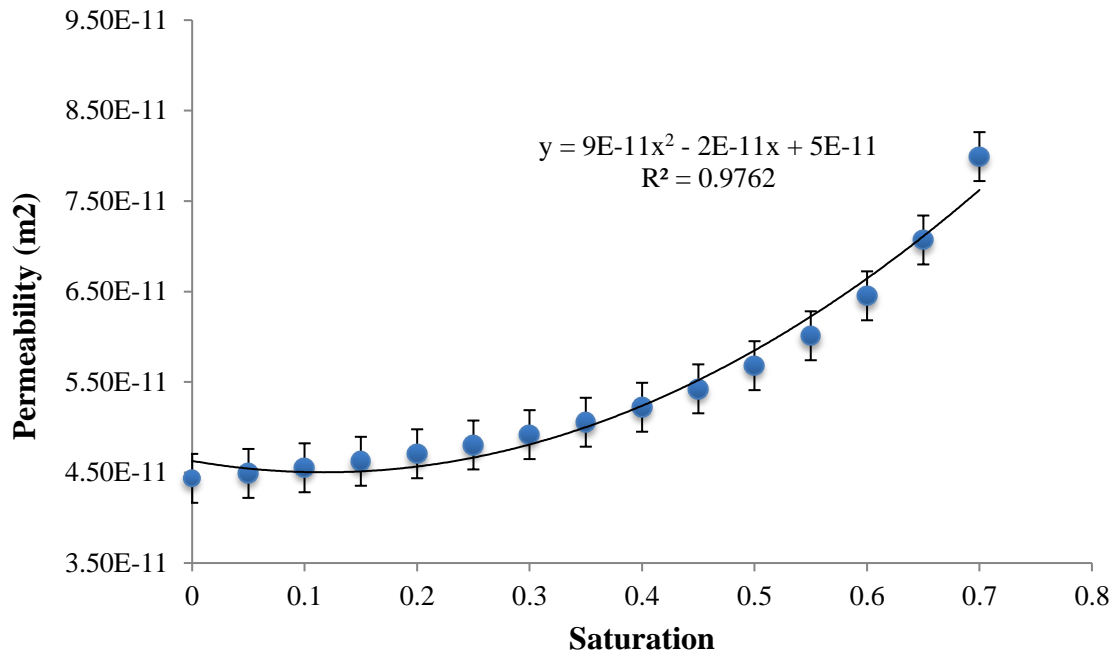
Figure 25.Permeability vs. saturation (Error bars: SE)

The best-fit curve gave a second-degree polynomial with an R^2 value of 0.97, which will also be plugged in the model. The results of fig. 25 can be compared to data on other porous media. For example, sands and gravel exhibit permeabilities in the range 10^{-11}-10^{-10} m^2 and are considered pervious[26]. Therefore, the results are physically reasonable.
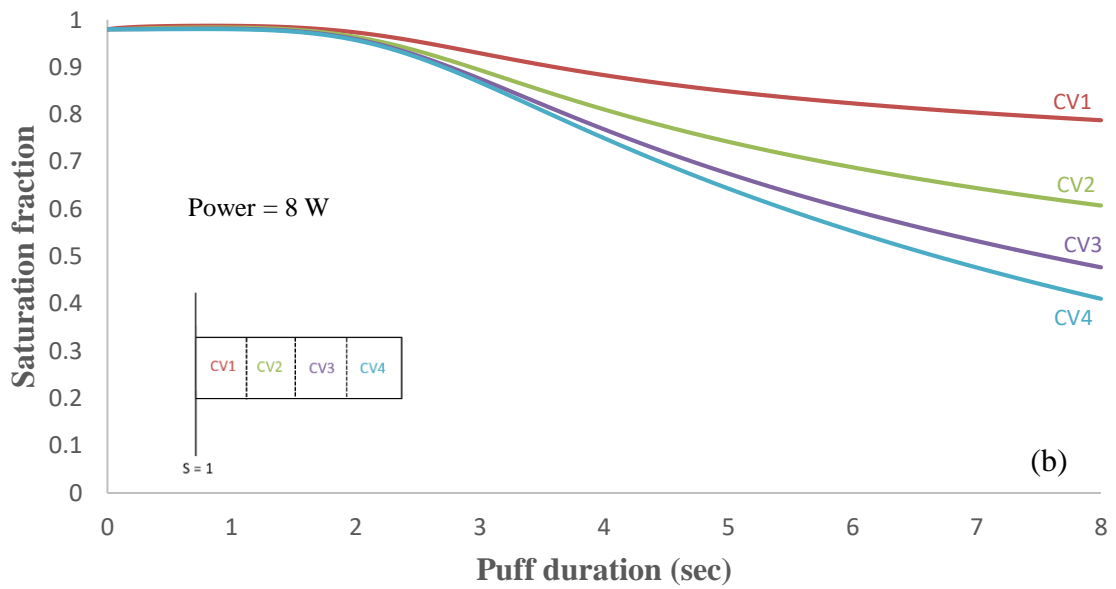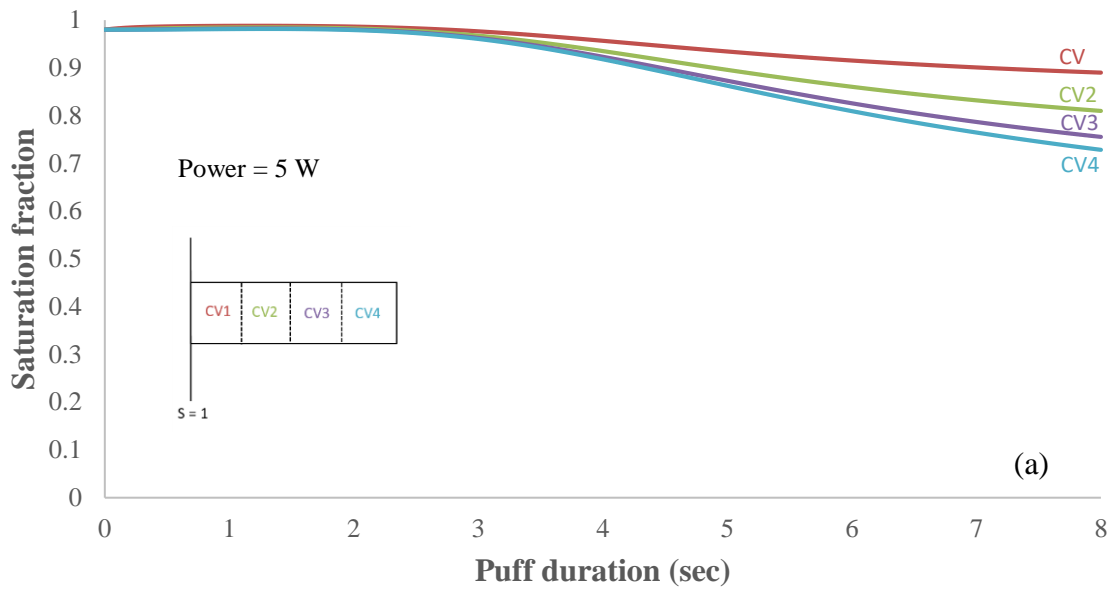
C. Model Simulation

In this section the effects of different operating conditions on saturation levels (S) are studied, where the resulted series of differential equations are numerically solved in Matlab® computing environment using a time-explicit algorithm in increments of 0.001 s, a coil length and diameter of 2 cm and 1 mm respectively, PG as the e-liquid and

Ekowool™ ($\epsilon = 0.7$) as the wicking material. For simplicity, four CVs are used to show the results; however, the user can choose up to 40 CVs.

1. *Effect of power input and puff duration.*

As shown in fig. 26, higher input power resulted in lower saturation levels. This is due to the fact that the electrical power input is directly proportional to heater coil temperature (Eq. 10), and the increase of coil temperature results in an increase of the liquid's vapor pressure and subsequently a higher $\dot{m}_{evap}$. The transient nature of the process is responsible for the delay interval shown in fig. 26 before saturation levels start dropping. When the heater coil is first energized, its temperature rises until the various thermal energy dissipation routes attain a rate that balances the rate at which electrical energy is input to the coil, the time taken to attain this steady state is a measure of the "thermal inertia" of the coil and its immediate surroundings[19]. A higher coil power resulted in a shorter delay interval, since energy is dissipated at a higher rate (fig. 26 (c)).

Power = 5 W

CV1 CV2 CV3 CV4

S = 1

CV
CV2
CV3
CV4

(a)

Power = 8 W

CV1 CV2 CV3 CV4

S = 1

CV1
CV2
CV3
CV4

(b)

Figure 26. Effect of power input on saturation levels (Wick diameter = 2 mm, Wick length = 2 cm, E-liquid: PG, Coil material: Kanthal, Coil diameter = 1 mm)

As shown in fig. 27, longer puffs resulted in lower saturations; this is also due to the transient nature of the process, where for shorter puff durations, a larger portion of the puff will fall in the transient state resulting in lower average evaporated e-liquid.
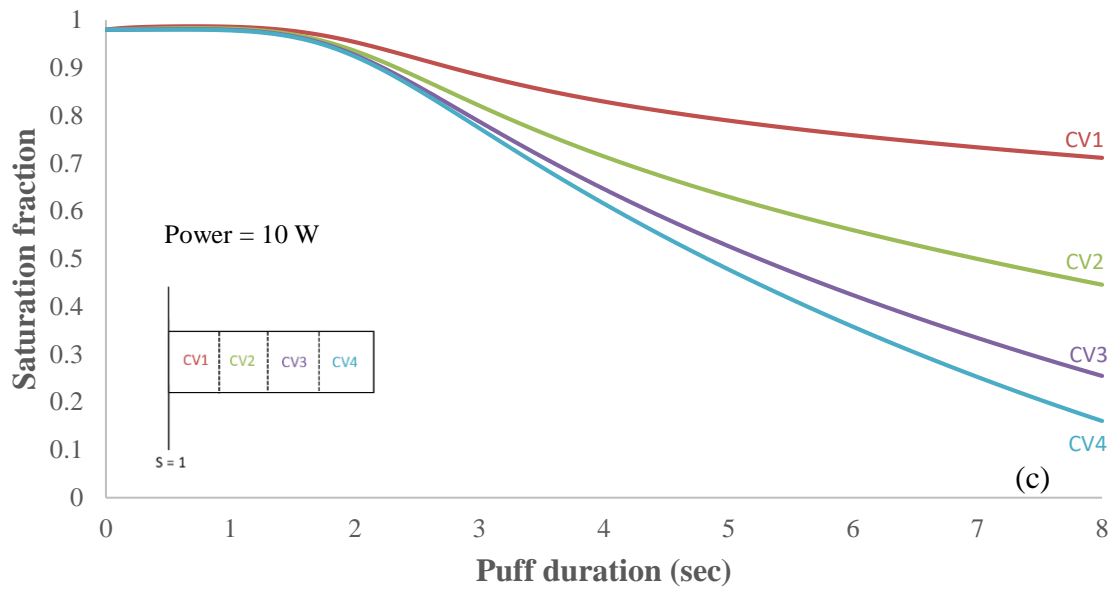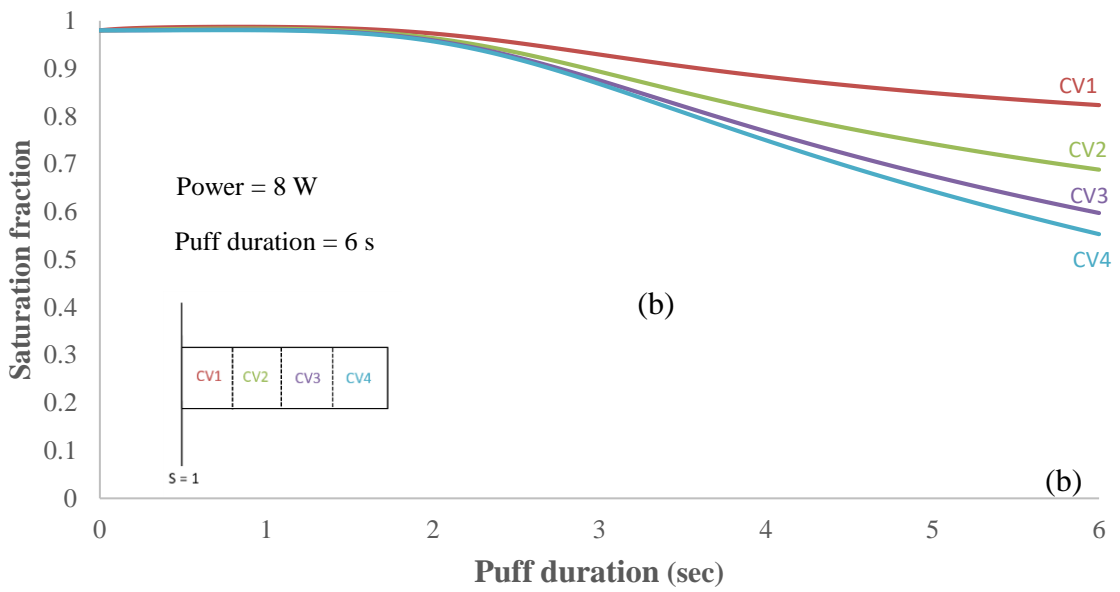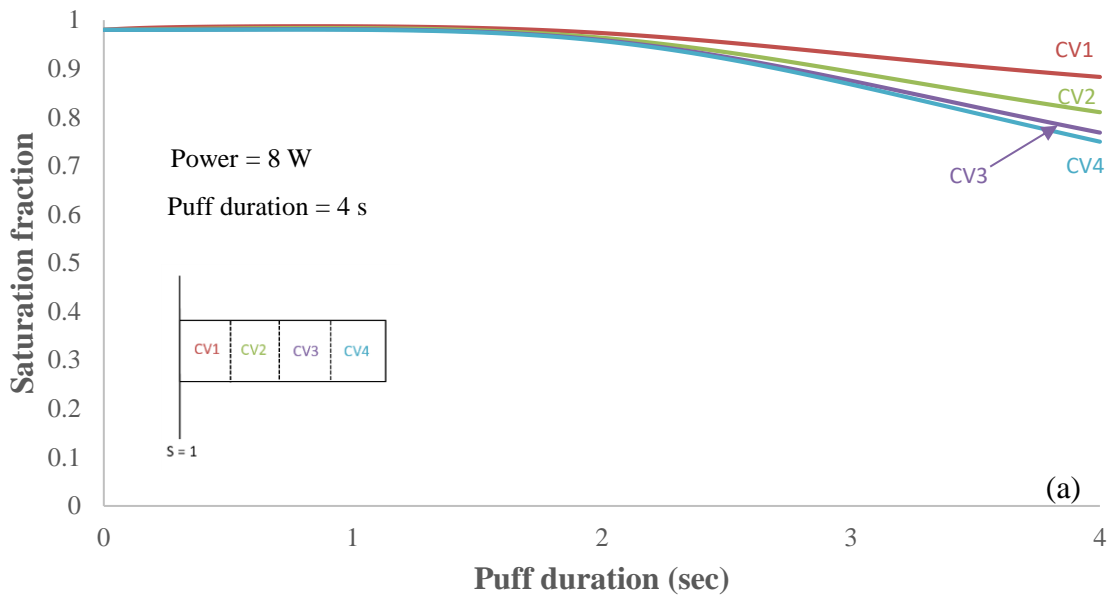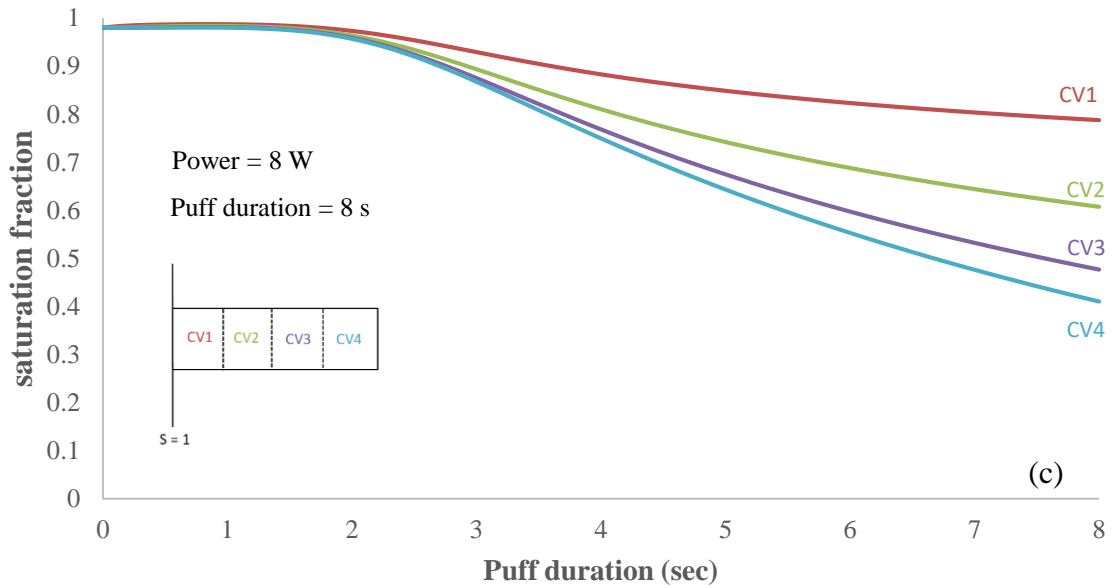
(a)

(b)

Figure 27. Effect of puff duration on saturation levels (Wick diameter = 2 mm, Wick length = 2 cm, E-liquid: PG, Coil material: Kanthal, Coil diameter = 1 mm)

2. *Effect of inter-puff duration.*

The inter-puff duration is the interval where the wick regains the vaporized liquid lost during a puff. It is an important factor since it determines the initial saturation of the succeeding puff. Fig. 28 shows the effect of inter-puff duration on CV 4 only at 4 (Fig. 28 (a)) and 10 (Fig. 28 (b)) watts for 10 consecutive puffs, the puff duration is 4 sec and the inter-puff durations are 4, 6 and 12 sec. In both figures, the wick exhibits a transient behavior for the first few puffs before reaching a steady state, it also regains more liquid during longer inter-puff durations. In Fig.28(a), the minimum and maximum steady state saturation levels are higher with longer inter-puff intervals, since the wick is recovering

more liquid. For example, the minimum saturation at steady state for 4 sec inter-puff interval is 0.83 while it is 0.87 for 12 sec inter-puff interval.
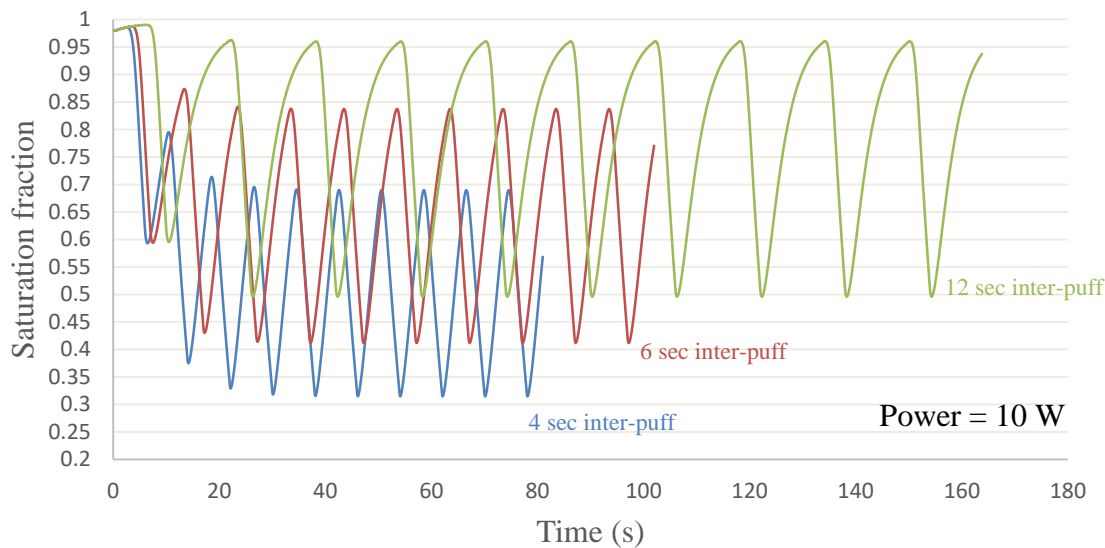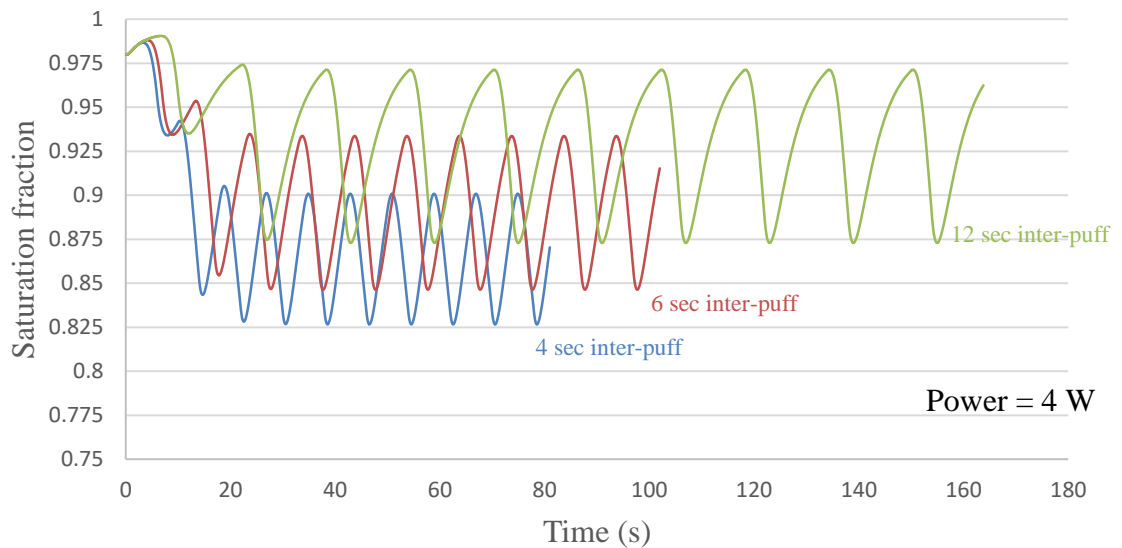

Figure 28. Effect of inter-puff durations (Wick diameter = 2 mm, Wick length = 2 cm, E-liquid: PG)

This difference is even greater in Fig.28(b) (10 watts), where the minimum saturation at 4 sec inter-puff is 0.31 and 0.5 for 12 sec inter-puff, since higher power

increase $\dot{m}_{evap}$ (section C.1) and subsequently decrease the overall saturation levels. It is

also noticed that the difference between the maximum and minimum saturation levels is

greater within the same inter-puff durations between 4 and 10 watts. For example, in 4 sec

inter-puffs, the difference between the maximum and minimum saturation levels at steady

state is 0.08 at 4 watts, while it is approximately 0.37 at 10 watts. This difference is due to

the very low saturation levels at the end of each puff at 10 watts, which increase the liquid

flow rate inside the wick since the flow rate is inversely proportional to saturation levels.

D. Model validation.

The transient nature of the problem makes it difficult to validate the model using a

real ECIG, since there are numerous ECIG designs and geometries with various thermal

masses. The "thermal inertia" interval varies widely depending on the thermal mass of the

device. Therefore, the model was validated based on the minimum saturation attained by a

single CV coil-wick unit, at this point the CV is at a steady state where the input energy is

only directed towards vaporizing the liquid in the wick. The minimum saturation in the CV

is also an important parameter in determining the temperature of the CV. As liquid

saturation decreases in the CV the input energy is dissipated more towards heating the CV

(e.g. increase in $\dot{Q}_{cond.}$) thus increasing its temperature.

The same experimental setup used to get the permeability was also used to validate

the model (fig. 20), the experiment was repeated with 10-sec puff duration at 2, 5,7 and 10

watts (n = 3). Figure 29 shows how the predicted minimum saturation is highly correlated

to the measured minimum saturation ($R^2 = 0.98$).
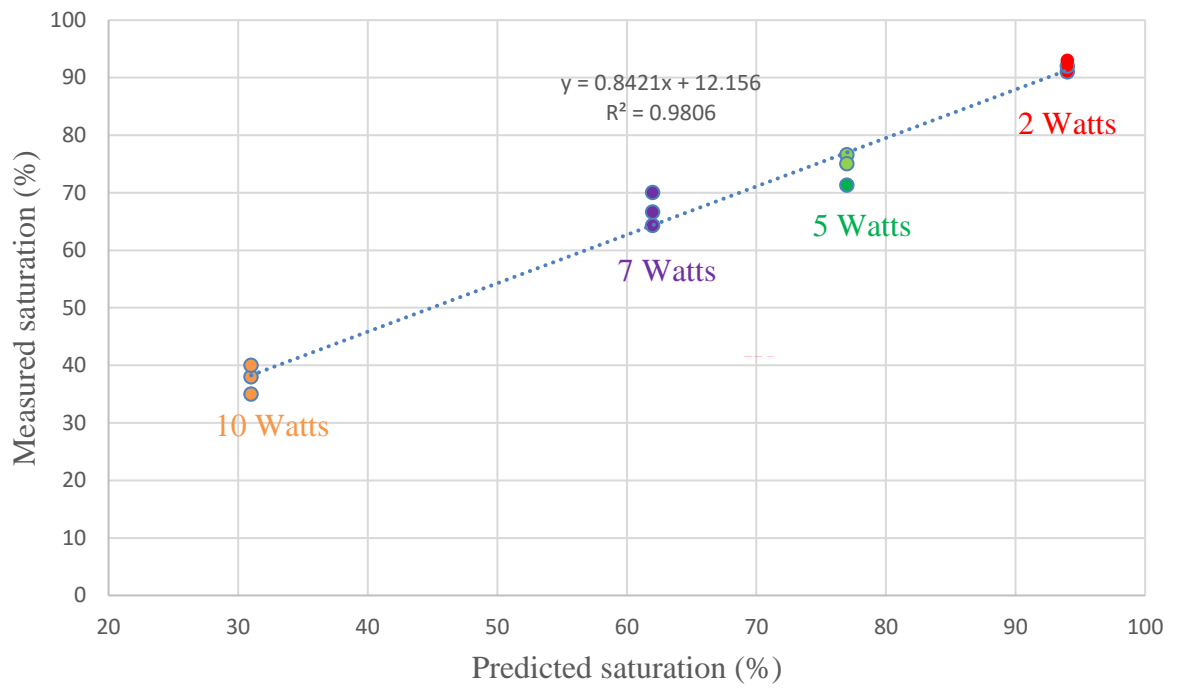
Figure 29.Measured vs. predicted minimum saturation

CHAPTER V

CONCLUSION

The mathematical model proved capable of predicting saturation levels, which is an important parameter that can be linked to aldehyde emissions through temperature. This was done for one type of wicking materials; however, a new method for determining the permeability as a function of liquid saturation was developed and can be applied on different wicking materials to get their wicking properties.

The mathematical model can be used to guide selection of materials, use conditions and product designs for subsequent human lab investigations. Correlating saturation levels with aldehyde emissions is key for the model to be effective. Aldehyde emissions reported in the literature can be related to saturation levels by running the code under the same operating conditions.

APPENDIX A

Thermo-physical properties of propylene glycol (PG) [33]

$$M_{PG} = 76.09 \times 10^{-3} \frac{kg}{mol}$$

$$T_b = 188°C$$

$$\rho_{PG} = 1.036 \times 10^3 \frac{kg}{m^3}$$

$$c_p = 2.5 \times 10^3 \, J/kg.K$$

$$\sigma = 36 \times 10^{-3} \, N/m$$

$$h_{fg,PG} = 914 \times 10^3 \, J/kg$$

$$K_{PG} = 0.206 \, W/m.K$$

$$\mu_{PG} = 0.0486 \, N.s/m^2$$

$$h_{m,PG} = 0.0387 \, m/s$$

Antoine equation was used to compute the vapor pressure of PG [34]:

$$\log_{10} P_v = A - \left(\frac{B}{T+C}\right) \qquad (A = 6.07936, B = 2692.187, C = -17.94)$$

APPENDIX B

The figure below shows the parameters that were extracted from the collected data to get saturation levels at steady state and permeability *(k)*.
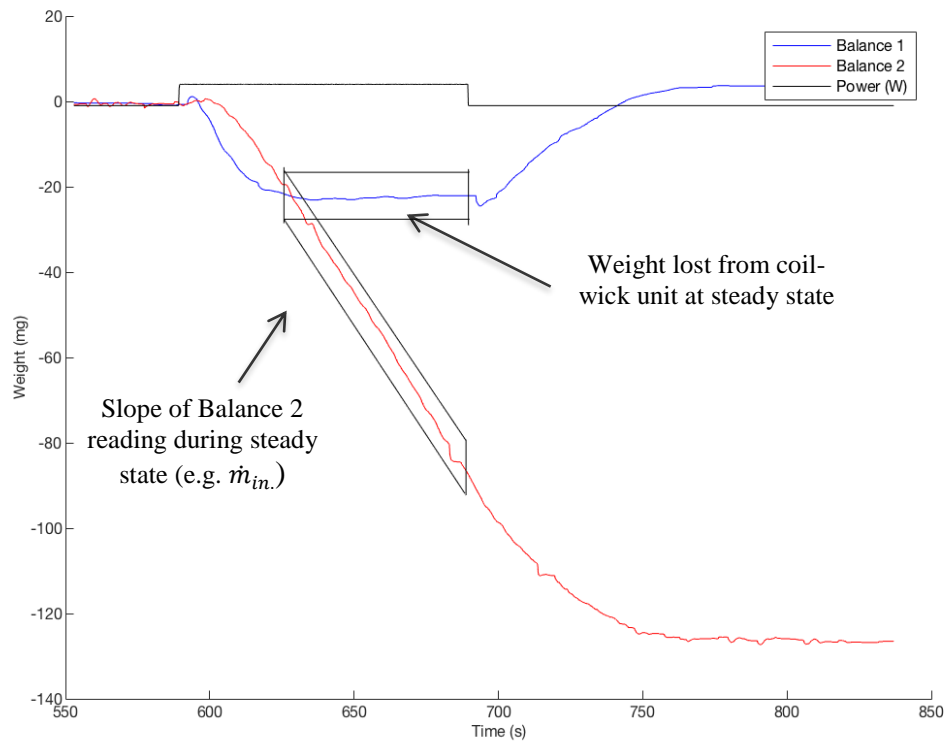
The tables below shows all the data collected at 3, 4 and 8 wraps. This data was used to get saturation levels and $\dot{m}_{in}$ at steady state in order to get the *k-S* relation.

At each power, the puff was repeated three times to reach steady state and average values were used.

3 Wraps:

Power (W)	Weight lost from coil-wick unit at steady state (mg)			Slope of Balance 2 reading during steady state ($\dot{m}_{in.}$) (mg/s)		
	Trial 1	Trial 2	Trial 3	Trial 1	Trial 2	Trial 3
1	-6	-6	-5	-0.302	-0.29	-0.3
1.5	-8.8	-7.9	-8.2	-0.51	-0.5	-0.51
2	-14.8	-15	-14.9	-0.73	-0.73	-0.74
3	-22.2	-22.1	-22.3	-1.01	-1.01	-1.01

8 Wraps:

Power (W)	Weight lost from coil-wick unit at steady state (mg)			Slope of Balance 2 reading during steady state ($\dot{m}_{evap.}$) (mg/s)		
	Trial 1	Trial 2	Trial 3	Trial 1	Trial 2	Trial 3
1	-6	-6.2	-5.8	-0.35	-0.36	-0.36
1.5	-14.6	-14	-14.6	-0.61	-0.61	-0.62
2	-24.4	-24.2	-25	-0.7	-0.71	-0.7

	Weight lost from coil-wick unit at steady state (mg)			Slope of Balance 2 reading during steady state ($\dot{m}_{evap.}$) (mg/s)		
3	-25.8	-25.7	-25.8	-0.75	-0.78	-0.78

4 Wraps:

Power (W)	Weight lost from coil-wick unit at steady state (mg)			Slope of Balance 2 reading during steady state ($\dot{m}_{evap.}$) (mg/s)		
	Trial 1	Trial 2	Trial 3	Trial 1	Trial 2	Trial 3
1	-5.8	-6.2	-5.2	-0.24	-0.22	-0.21
1.5	-5.5	-5.5	-6.2	-0.43	-0.45	-0.42
2	-7.4	-7	-6.5	-0.64	-0.66	-0.66
3	-8.5	-8.7	-8.7	-1.1	-1.04	-1.05

BIBLIOGRAPHY

[1]   O. Rom, A. Pecorelli, G. Valacchi, and A. Z. Reznick, "Are E‑cigarettes a safe and good alternative to cigarette smoking?," *Annals of the New York Academy of Sciences,* vol. 1340, no. 1, pp. 65-74, 2015.

[2]   "Electronic cigarettes (e-cigarettes) dollar sales worldwide from 2008 to 2017 (in million U.S. dollars)*," Agora Financial2014.

[3]   J. Foulds, S. Veldheer, and A. Berg, "Electronic cigarettes (e‑cigs): views of aficionados and clinical/public health perspectives," *International journal of clinical practice,* vol. 65, no. 10, pp. 1037-1042, 2011.

[4]   A. McQueen, S. Tower, and W. Sumner, "Interviews with "vapers": implications for future research with electronic cigarettes," *Nicotine & Tobacco Research,* vol. 13, no. 9, pp. 860-867, 2011.

[5]   A. Breland, E. Soule, A. Lopez, C. Ramôa, A. El‑Hellani, and T. Eissenberg, "Electronic cigarettes: what are they and what do they do?," *Annals of the New York Academy of Sciences,* vol. 1394, no. 1, pp. 5-30, 2017.

[6]   T. Singh, "Tobacco use among middle and high school students—United States, 2011–2015," *MMWR. Morbidity and mortality weekly report,* vol. 65, 2016.

[7]   D. Nikitin, D. S. Timberlake, and R. S. Williams, "Is the e-liquid industry regulating itself? A look at e-liquid Internet vendors in the United States," *Nicotine & Tobacco Research,* vol. 18, no. 10, pp. 1967-1972, 2016.

[8]   J. Phua, Jin, S., Hahm, JM., "Celebrity-endorsed e-cigarette brand Instagram advertisements: Effects on young adults' attitudes towards e-cigarettes and smoking intentions.," *J Health Psychol,* pp. 550-560, 2018.

[9]   J. F. E. a. C. Bullen, "Electronic cigarette: users profile, utilization, satisfaction and perceived efficacy," *Addiction,* pp. 2017-2028, 2011.

[10]   L. R. K. Schaller, S. Kahnert, C. Bethke, U. Nair and M. Potschke-Langer, "Electronic Cigarettes - an Overview," Tobacco Prevention and Tobacco Control Heidelberg 2013.

[11]   T. K. M. L. Goniewicz, M. Gawron, J. Knysak and L. Kosmider, "Nicotine Levels in Electronic Cigarettes," *Nicotine & Tobacco Research,* 2012.

[12]   L. S. Bahl V, Xu N, Davis B, Wang YH & Talbot P, "Comparison of electronic cigarette refill fluid cytotoxicity using embryonic and adult models.," *Reprod Toxicol,* pp. 529-537, 2012.

[13]   !!! INVALID CITATION !!! (Jensen, 2015; Kanae, 2014 ; Uchiyama, 2013).

[14]   D. Hoffmann, Adams, JD., Lisk, D., Fisenne, I., Brunnemann, KD., "Toxic and carcinogenic agents in dry and moist snuff.," *J Natl Cancer Inst. ,* 1987.

[15]   "Agents classified by the IARC monographs," http://monographs.iarc.fr/2013.

[16] P. Jensen, Luo, W., Pankow, J., Strongin, R., Peyton, D., "Hidden Formaldehyde in E-Cigarette Aerosols," The New England Journal of Medicine2015.

[17] A. S. L. Kosmider, M. Fik, J. Knysak.,M. Zaciera., J. Kurek., ML. Goniewicz, "Carbonyl compounds in electronic cigarette vapors: effects of nicotine solvent and battery output voltage.," *Nicotine Tob Res.,* vol. 16, no. 10, pp. 1319-26, 2014.

[18] Z. Balhas, Talih, S., Eissenberg, T., Salman, R., Karaoghlanian, N., Shihadeh, A .,, "Effects of user puff topography and device characteristics on electronic cigarette nicotine yield.," 2014.

[19] B. Z. Talih S., Salman R., El-Hage R., Karaoghlanian N., El-Hellani A., Baassiri M., Jaroudi E., Eissenberg T., Saliba N., Shihadeh A., "Transport phenomena governing nicotine emissions from electronic cigarettes: Model formulation and experimental investigation," *Aerosol Science and Technology,* vol. 51, pp. 1-11, 2017.

[20] J.-M. Marchal, "Modeling Capillary Flow in Complex Geometries," *Textile Research Journal,* pp. 813-821, 2001.

[21] F. A. L. Dullien, *Porous Media: Fluid Transport and Pore Structure*. London: Academic Press, 1992.

[22] P. G. Tortora, Collier, B. J., *Understanding Textiles*. Upper Saddle River, NJ Prentice-Hall, Inc., 1997.

[23] M. Kutílek, Nielsen, D., *Soil hydrology*. Catena , Cremlingen, 1994.

[24] D. Nield, Bejan, A., *Convection in Porous Media*. Springer, 2006.

[25] J. Bear, Bachmat, Y., *Introduction to Modeling of Transport Phenomena in Porous Media*. 1990.

[26] J. Bear, *Dynamics of fluids in porous media*. Amsterdam: Elsevier, 1972.

[27] M. Hassanizadeh, Gray, W., "General conservation equations for multi-phase systems," *Advances inWater Resources,* pp. 25-40, 1980.

[28] Malay K. Das, Partha P. Mukherjee, and K. Muralidhar, *Modeling Transport Phenomena in Porous Media with Applications*. Springer International Publishing, 2018, pp. XI, 241.

[29] M. Muskat, Wyckoff, H. G., Botset, M. W., Meres, M. W., *Transactions of the Metallurgical Society of AIME,* 1937.

[30] K. Ghali, Jones, B., Tracy, J., "Modeling heat and mass transfer in fabrics " *Int. J. Heat Mass Tranfer,* pp. 13-21, 1995.

[31] N. Malek, Nakkash, R., Talih, S., Lotfi, T., Salman, R., Karaoghlanian, N., El-Hage, R., Saliba, N., Eissenberg, T., Shihadeh, A., "A Transdisciplinary Approach to Understanding Characteristics of Electronic Cigarettes," *Tobacco Regulatory Science,* vol. 4, pp. 47-72, 2018.

[32] K. Ghali, Jones, B., Tracy, J., "Experimental Techniques for Measuring Parameters Describing Wetting and Wicking in Fabrics," *Textile Research Journal,* pp. 106-111, 1994.

[33] N. C. f. B. Information. [Online]. Available: https://pubchem.ncbi.nlm.nih.gov/compound/1030.

[34]   D. R. Stull, "Vapor Pressure of Pure Substances. Organic and Inorganic Compounds," *Ind. Eng. Chem.,* pp. 517-540, 1947.